Advanced Drug Delivery Reviews 143 (2019) 97–114

Contents lists available at ScienceDirect

Advanced Drug Delivery Reviews

journal homepage: www.elsevier.com/locate/addr

Absorption, distribution, metabolism and excretion of the biomaterials used in Nanocarrier drug delivery systems

Chong Su [a,b], Yingze Liu [a,b,c], Runzhi Li [a,b], Wei Wu [d], John Paul Fawcett [a,b], Jingkai Gu [a,b,*]

[a] Research Center for Drug Metabolism, School of Life Sciences, Jilin University, Changchun, 130012, PR China
[b] Beijing Institute of Drug Metabolism, Beijing 102209, PR China
[c] School of Pharmaceutical Sciences, Jilin University, Changchun 130012, PR China
[d] Key Laboratory of Smart Drug Delivery of MOE, School of Pharmacy, Fudan University, Shanghai 201203, China

ARTICLE INFO

Article history:
Received 23 December 2018
Received in revised form 16 June 2019
Accepted 25 June 2019
Available online 28 June 2019

Keywords:
Drug delivery systems
Nanocarriers
Nanoparticles
Bioassay
Pharmacokinetics
Pharmacodynamics

ABSTRACT

Nanocarriers (NCs) are a type of drug delivery system commonly used to regulate the pharmacokinetic and pharmacodynamic properties of drugs. Although a wide variety of NCs has been developed, relatively few have been registered for clinical trials and even fewer are clinically approved. Overt or potential toxicity, indistinct mechanisms of drug release and unsatisfactory pharmacokinetic behavior all contribute to their high failure rate during preclinical and clinical testing. These negative characteristics are not only due to the NCs themselves but also to the materials of the drug nanocarrier system (MDNS) that are released in vivo. In this article, we review the main analytical techniques used for bioassay of NCs and MDNS and their pharmacokinetics after administration by various routes. We anticipate our review will serve to improve the understanding of MDNS pharmacokinetics and facilitate the development of NC drug delivery systems.

Contents

Abbreviations: ADME, absorption distribution metabolism excretion; CD, cyclodextrin; CNTs, carbon nanotubes; DDS, drug delivery systems; EPR, enhanced permeability and retention; EO, ethylene oxide; FITC, fluorescein isothiocyanate; GI, gastrointestinal; GPC-RI, gel permeation chromatography-refractive index detection; HA, hyaluronic acid; LC-MS/MS, liquid chromatography tandem mass spectrometry; LLOQ, lower limit of quantitation; MDNS, materials of the drug nanocarrier system; MPS, mononuclear phagocyte system; MRI, magnetic resonance imaging; NC, nanocarrier; NP, nanoparticle; PCL, polycaprolactone; PD, pharmacodynamics; PEG, poly(ethylene glycol); PK, pharmacokinetics; PLA, poly(lactic acid); PLGA, poly(lactic-*co*-glycolic acid); PO, propylene oxide; PVA, poly(vinyl alcohol); PVP, polyvinylpyrrolidone; SF, silk fibroin.

* Corresponding author at: Research Center for Drug Metabolism, School of Life Sciences, Jilin University, Changchun 130012, PR China.
E-mail address: gujk@jlu.edu.cn (J. Gu).

https://doi.org/10.1016/j.addr.2019.06.008
0169-409X/

1. Introduction

During the last two decades, great advances have been made in the development of nanocarrier (NC) drug delivery systems (DDS) thereby providing new opportunities in formulation design [1,2]. The use of NCs is a strategy for selective delivery of therapeutic small drug molecules and genes to target cells of interest [3,4]. They can take various forms including polymers, dendrimer nanoparticles (NPs), liposomes, micelles, hydrogels, metallic, magnetic and semiconductor NPs and carbon nanotubes (CNTs) (Fig. 1) [3]. They are generally superior to the more traditional drug delivery vehicles because of their capacity to overcome many of the current limitations in the pharmacotherapy of human disease [5].

NCs have controllable surface characteristics that provide the ability to regulate drug release [6]. In this way, NCs can modify the pharmacokinetics (PK) and pharmacodynamics (PD) of payload drugs and

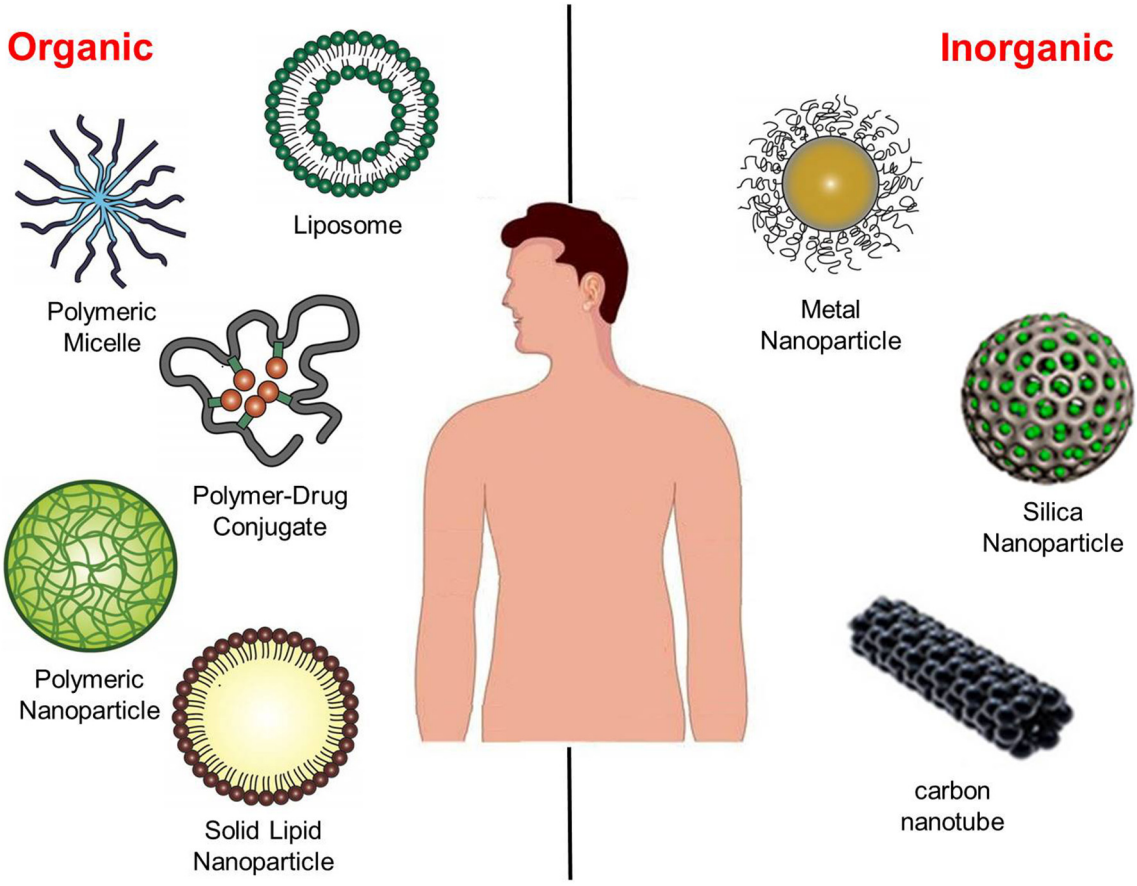

Fig. 1. Summary of the various categories of nanocarrier.

potentially improve their therapeutic effects [7]. In addition, loading drugs into NCs can improve their in vivo stability, prolong their blood circulation time and, in the case of anticancer drugs, facilitate their uptake by tumors with the help of the enhanced permeability and retention (EPR) effect [7]. Despite these benefits and the thousands of publications related to NCs, only a small number of NC-based formulations has been approved for clinical use (e.g. Doxil®, Caelyx®, Myocet® and Abraxane®) or registered for clinical trials. This indicates a big gap between the technical and clinical development of NC DDS [7].

As stated above, potential toxicity, indistinct mechanisms of action and unsatisfactory PK are important reasons for the high failure rate of NCs during clinical development [1]. A typical NC contains a significant portion of carrier and/or encapsulation material which, when released in vivo through dissociation, leakage or breakdown, gives rise to materials of the drug nanocarrier system (MDNS). MDNS generally have excellent biocompatible, mechanical and stable properties, and can control and sustain drug release, facilitate EPR effects and promote uptake of drug by cancer cell lines. As xenobiotics, MDNS can exhibit systemic toxicity, be converted to toxic metabolites or accumulate in certain vital organs or tissues with potential toxicological effects. In addition, MDNS may interact with drug transporters to modulate drug distribution and/or give rise to drug-MDNS interactions.

There are numerous MDNS-mediated deleterious effects, for instance: Poly(ethylene glycol) (PEG) can accumulate in tissues [8], act as a P-gp inhibitor [9–13] and produce an acid metabolite implicated in causing acidosis and hypercalcemia [14]; poly(lactic acid) (PLA) and poly (lactic-*co*-glycolic acid) (PLGA) can lead to inflammatory responses [15,16]; polyvinylpyrrolidone (PVP) can accumulate in human tissues when administered parenterally and cause harmful effects [17]; derivatives of cyclodextrins (CDs) can cause toxicity to the kidney, intestine and lung [18–20]; chitosan can facilitate platelet adhesion and reduce the absorption of fat from the gastrointestinal (GI) tract [21,22]; poloxamer can lead to renal dysfunction [23]; inorganic-based MDNS such as those produced from metallic NPs, CNTs and silicon-based NPs (SiNPs) can damage organs [24–26] and DNA [27,28] and give rise to oxidative stress [29,30], apoptosis [31–33] and inflammation [34–36].

Clearly, understanding the in vivo fate of MDNS viz. their absorption, distribution, metabolism and excretion (ADME, Fig. 2) is significant in evaluating the overall safety and promoting the development of NC DDS [37]. However, achieving this understanding has been limited by the lack of bioassays for MDNS capable of providing comprehensive PK information. This lack is partly due to the complexity of MDNS and the susceptibility of relevant analytical methods to be limited by significant interference from endogenous molecules.

NCs incorporate a wide range of MDNS in their preparation [7]. In this review, we have concentrated on the following common MDNS (Fig. 3): Polyesters [PLA, PLGA, polycaprolactone (PCL)]; PEGs and PEG-associated derivatives; polysaccharides [chitosan and hyaluronic acid (HA)]; polyenes [poly(vinyl alcohol) (PVA), PVP)]; proteins [silk fibroin (SF)] and cyclodextrins (CDs). Data relating to their PK are summarized in Table 1. This review first describes the bioanalytical methods used to determine MDNS and their advantages and disadvantages.

2. Bioassay of MDNS

At present, common methods for the bioassay of MDNS are fluorescence imaging, radioisotope labeling, gel permeation chromatography with refractive index detection (GPC-RI), magnetic resonance imaging (MRI), ICP-MS and LC-MS/MS (Table 2). These methods have respective merits such as: good selectivity, high sensitivity, and excellent accuracy. They are therefore suitable for use in PK studies of MDNS.

2.1. Fluorescence labeling

Fluorescence labeling has been widely used to determine MDNS because it combines high sensitivity with cost-effectiveness and non-invasiveness [38,39]. For example, Schadlich et al. investigated the distribution, accumulation and elimination of PVA after intraperitoneal (i.p.) administration to mice [40] (Fig. 4, I) of PVA labeled with either rhodamine dye or Alexa Fluor 750. Preparation of the PVA-rhodamine dye was reported in a previous study [41]. Labelling with Alexa Fluor 750 involves five steps viz. decrystallization, tosylation, azidation, amination, and Alexa Fluor 750 conjugation. Wen et al. used fluorescence labelling to evaluate the influence of molecular weight (MW) on the PK behavior of carboxymethylchitosan [42]. The analyte was labeled with fluorescein isothiocyanate (FITC) via reaction between its isothiocyanate group and the primary amino group of chitosan. Kuehl et al. used fluorescence imaging to study the dependence of HA MW on its clearance and biodistribution from mouse lung using HA labeled with the near

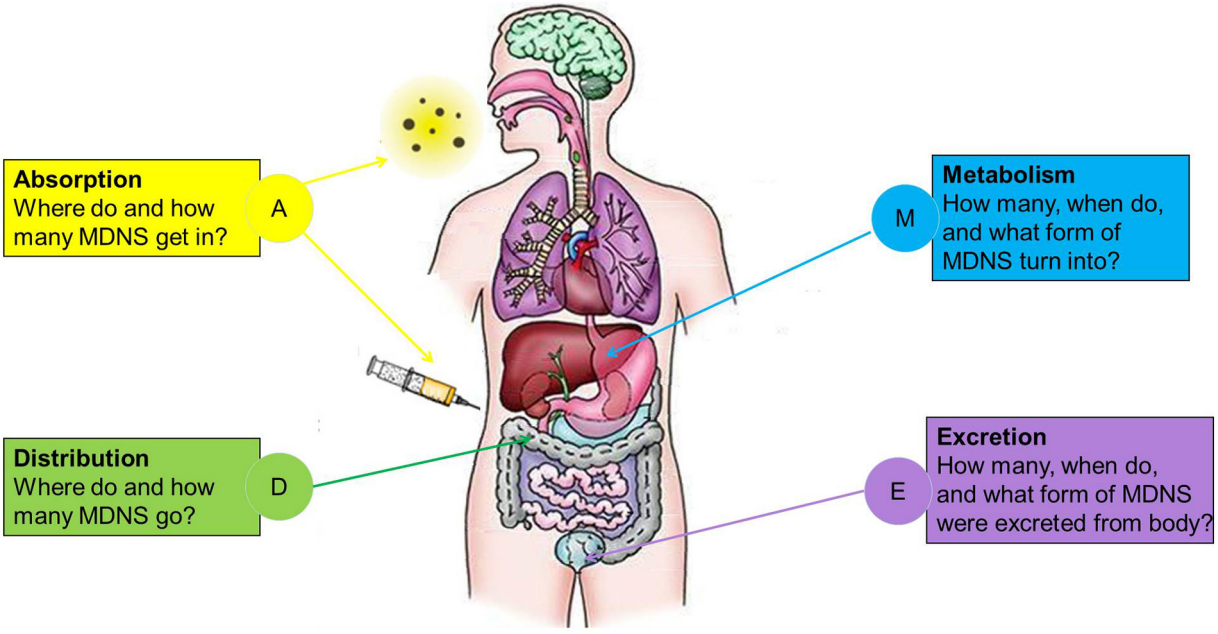

Fig. 2. ADME processes of MDNS in vivo. (A: absorption; D: distribution; E: excretion; M: metabolism; MDNS: materials of the drug nanocarrier system)

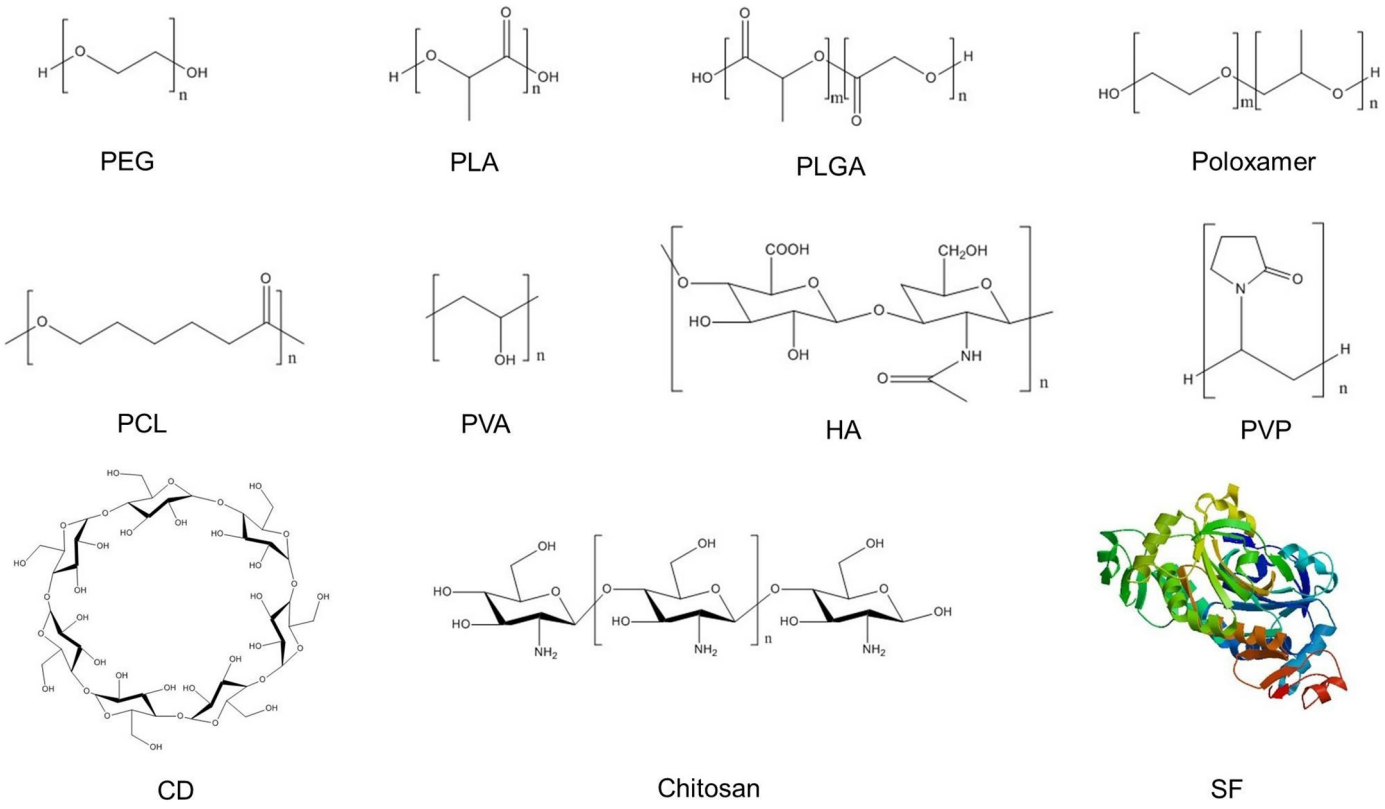

Fig. 3. Structures of MDNS. (CD: cyclodextrin; CNT: carbon nanotube; HA: hyaluronic acid; PCL: polycaprolactone; PEG: poly(ethylene glycol); PLA: poly(lactic acid); PLGA: poly(lactic-*co*-glycolic acid); PVA: poly(vinyl alcohol); PVP: polyvinylpyrrolidone; SF: silk fibroin)

infrared dye, 750 hydrazide [43] (Fig. 4, II). The labeling process of HA was described in earlier studies [44–46] where the authors showed that the conjugation efficiency decreased as MW of HA increased.

The main problem with using fluorescent dyes to visualize analytes is to ensure that the fluorescent label remains bound to the analyte [47]. While this is best achieved through covalent binding, it can change the physicochemical properties of the analyte such as its solubility or hydrophobic–hydrophilic balance leading to misleading PK results. Moreover, fluorescence can be quenched or degraded, and fluorescent light cannot penetrate thick tissues. It is also difficult to investigate the metabolism of fluorescence labeled MDNS because fluorescent dyes are likely to be cleaved by metabolic processes. Fluorescent reagents can also exhibit toxicity to living organisms that can limit their clinical application.

2.2. Radiolabeling

Radiolabeling an analyte with an isotopic tracer allows its determination with excellent accuracy, high sensitivity and low interference [48]. As a result, radiolabeling has been extensively applied to investigate the PK of MDNS. For instance, Longley et al. radiolabeled 40 kDa PEG with ^{14}C and investigated its PK following intravenous (i.v.) administration to mice [8]. The ^{14}C label was attached to the ether bonds of PEG so that the radioactivity was emitted by the entire PEG molecule. With the similar method, Grindel et al. investigated the distribution of ^{14}C-labeled poloxamer 188 in rats, dogs and humans [49].

The preclinical PK of HA was investigated by radiolabeling it with ^{99m}Tc and ^{14}C [50,51] (Fig. 5, I). Labeling with ^{99m}Tc used a direct method whereas ^{14}C labeling was achieved by fermentation through cultivating *Streptococcus* in a ^{14}C-glucose culture medium as described in an earlier study [52]. Laznicek et al evaluated the stability of the labels in different solvents and, although they found ^{14}C-HA was more stable than ^{99m}Tc-HA, both labels were suitable for short duration biodistribution studies. Balogh et al also prepared ^{99m}Tc-HA using a direct labeling method [51].

Alric et al. investigated the biodistribution of AuNPs radiolabeled with ^{99m}Tc and ^{111}In [53] (Fig. 5, II) in the dithiolated polyaminocarboxylate shell. Introduction of the ^{99m}Tc-label was achieved by reducing pertechnetate $^{99m}TcO_4$ with stannous chloride in the presence of the AuNPs whereas the ^{111}In-label was introduced simply by mixing AuNPs with ^{111}In–chloride in buffer solution. Hwang et al. studied the distribution and excretion of ^{131}I-labeled chitosan after injection to tumor-bearing rats [54]; they showed ^{131}I-labeled chitosan remained stable for up to 7 days.

In spite of wide application, the bioassay of a particular MDNS by radiolabeling may be compromised by instability of the label in vivo [48]. A direct way to overcome this is to incorporate the radioisotope into the MDNS during its synthesis. However, radioisotopes may alter the physicochemical properties of MDNS and change their PK behavior. In addition, radioisotopes may be released in the process of metabolism. Safety concerns are also important in using radiolabeled analytes and specially trained and experienced personnel are needed to handle them. Another limitation applies to the simultaneous use of several radioisotopes because of the low energy resolution of detection methods [39].

2.3. MRI

High spatial resolution of MRI makes it a valuable method to study the in vivo fate of NC DDS. Several researchers have applied MRI to tracing MDNS in vivo. Becker et al. used it to evaluate the tissue distribution of HA after subdermal injection for the correction of facial lipoatrophy in HIV-infected males [55]. Before the study, MRI detection parameters including axial T1 and T2 Dixon sequences, a T2 SPACE sequence and second T1 sequence, were optimized to achieve high accuracy. Biodistribution of HA was described using an anatomical classification

Table 1
Summary of ADME information for organic MDNS.

	Administration routes	Animal model	Absorption	Distribution	Metabolism	Excretion
PEG	Parenteral administration [126,127]; Oral administration [132,133]; Transdermal administration [134]; i.v. injection [8,135,138,139,142]	Rat [131,136,139]; Human [132,133,142]; Mice [8,136,138]; Guinea pig. [14]; Cat [14]; Rabbit [14]; Dog [142]	Absorbed by GI tract and skin; MW dependent	Distributes to kidney, lung, heart, liver, GI tract, spleen, and gall bladder after intravenous injection	Metabolized to carboxylic acid and sulfated metabolites by alcohol dehydrogenase and sulfotransferases respectively	Excreted in both bile and urine after intravenous injection; urinary clearance is probably the major pathway
PLA					Degraded by hydrolysis of ester bonds to lactic acid which enters the Krebs cycle to be metabolized to H_2O and CO_2.	N/A
PLGA	Oral administration [115,117]; Transdermal administration [116]; i.v. administration [60]	Rat [115]; Mice [117]	PLGA-nanoparticles can be absorbed after oral administration	Distributes to epidermis and dermis after treating human skin with microneedles; can distribute to spleen, kidney, intestine, liver, lung, brain and heart after oral administration	Undergoes hydrolysis to produce lactic acid and glycolic acid, and either of them can get into the Krebs cycle and be degraded to H_2O and CO_2	N/A
PVA	i.p. administration [41,182]; Intramuscular administration [182]; s.c. administration [182]; i.v. administration [194]	Rat [182]; Mice [182]	PVA absorption into the blood from different injection sites decreased in the order i.p. > intramuscular > s.c	Distributes to liver, GI tract and spleen after intravenous injection; can distribute to body fat tissues and liver after intraperitoneal injection	No metabolite has been observed	Excreted in both urine and feces after intravenous injection with urinary excretion the main pathway
PVP	Oral administration [187]; Parenteral administration [188]; i.v. injection [197–199]	Pig [187]	Absorbed from GI tract after oral administration	Distributes to omental fat, bone marrow, skin, muscle, nerve tissue, lung, ovary and liver	N/A	Excreted via both feces and urine after intravenous injection
Poloxamer	i.v. injection [49,57]	Dog, [49,59]; Rat [49,59]; Human [49,57,59]	N/A	Distributes to GI tract, kidney, lymph nodes, adrenal gland, salivary gland, thyroid gland, liver, lung, bone marrow, urinary bladder, ovaries, and spleen after intravenous injection	Metabolized to block copolymer	Excreted in both urine and feces after intravenous injection with urinary excretion the main pathway
CD	Oral administration [216,217]; i.v. administration [215]	Rat [214]	Absorbed from GI tract by passive diffusion; low absorption level (< 1%)	Distributes mainly to the kidney and to a lesser extent to bladder, liver and adrenal gland after oral administration	Metabolized in the GI tract mainly by bacterial digestion to produce oligosaccharides, monosaccharides and gases such as hydrogen, carbon dioxide and methane	Intravenously administered CDs rapidly excreted intact via the kidney; orally administered CDs excreted via urine
PCL	Subcutaneous injection [114]	Rat [114]	Absorbed after subcutaneous injection	N/A	Degraded by the hydrolysis of ester linkages via esterases	Excreted in feces and urine in rat after subcutaneous injection
Chitosan	i.p. administration [42,148,160,174]; oral administration [162,163]; i.v. administration [171,178]	Mice [160,171,178]; Rat [42,148,166,178]	Can be absorbed after intraperitoneal and oral administration; MW dependent	Distributes to kidney, liver, spleen, genitals, small intestine, plasma, lung, intestine, stomach, heart, muscle and brain after intravenous administration; to liver, spleen and kidney after intraperitoneal administration; to liver, stomach and muscle after hepatic artery injection	Enzymes can degrade chitosan by hydrolyzing bonds between glucosamines, *N*-acetylglucosamines and each other	Can be excreted in both urine and feces after intravenous administration; urinary excretion is the major pathway after intraperitoneal administration
Silk fibroin			N/A	N/A	Can be degraded by proteolytic enzymes into amino acids in vivo	N/A
Hyaluronic acid	Oral administration [50,51,164]; i.v injection [172,179]; Pulmonary administration [43]	Rat [50,164]; Mice [43,172]; Dog [51]; Rabbit [179]	Can be absorbed from GI tract	Distributes to kidney, spleen, liver, bone marrow after intravenous administration; to skin, GI tract, pancreas, harderian gland, liver, mandibular gland, joints, bone and muscle after oral administration; to lung and GI tract after pulmonary administration	Hyaluronidases can hydrolyze linkages between *N*-acetyl-D-glucosamine and D-glucuronic acid after which further degradation leads ultimately to CO_2, H_2O and urea	Excreted via respiration and in urine and feces after oral administration; excreted via respiration and in urine after intravenous injection

(ADME: absorption distribution metabolism excretion; CD: cyclodextrin; GI: gastrointestinal; i.p.: intraperitoneal; i.v.: intravenous; MDNS: materials of the drug nanocarrier system; MW: molecular weight; PCL: polycaprolactone; PEG: polyethylene glycol; PLA: polylactic acid; PLGA: poly (lactic-co-glycolic acid); PVA: poly(vinyl alcohol); PVA: poly(vinyl alcohol); PVP: polyvinylpyrrolidone; s.c.: subcutaneous; SF: silk fibroin).

Table 2
Analytical methods and their characteristics for the bioanalysis of MDNS.

Method	Merits	Defects
Fluorescence labeling	1. Economical	1. Fluorescence can be quenched or degraded in vivo
	2.Non-invasive	2. Fluorescent reagents may have toxicity
	3. Sensitive	3. Labeling reagent may alter the in vivo fate of MDNS
		4. MDNS degradation may result in false positive results
		5. Fluorescent light cannot penetrate thick tissue
Radiolabeling	1. Sensitive	1. Complicated operation
	2. Good selectivity	2. Cannot detect several radioisotopes at the same time
		3. Labeling reagent may alter the in vivo fate of MDNS
		4. Radioactivity is hazardous
		5. If material degrades in vivo, nuclide may lead to false positive result
MRI	1. Sensitive	1. Poor selectivity
	2. Non-invasive	2. Contrast agents are likely to alter the in vivo fate of MDNS
	3. Excellent space resolution	3. Cannot investigate the metabolism of MDNS
GPC-RI	1. High sensitivity for saccharides	1. Biological matrix may cause interference
	2. Good stability	2. GPC-RI is sensitive to temperature and mobile phase
	3. Convenient operation	
ICP-MS	1. Good selectivity	1. Endogenous metals in biological samples can cause strong interference
	2. Sensitive	2. Complex composition of biological samples may result in serious matrix effects
	3. Excellent accuracy	3. Sample preparation is complicated and time-consuming
LC-MS/MS	1. Good selectivity	1. Difficult to analyze MDNS that are polydisperse
	2. Sensitive	
	3. Excellent accuracy	

(GPC-RI: gel permeation chromatography with refractive index detection; ICP-MS: inductively coupled plasma mass spectrometry; LC-MS/MS: liquid chromatography tandem mass spectrometry; MDNS: materials of the drug nanocarrier system; MRI: magnetic resonance imaging).

reported in an earlier study [56]. SF and cellulose can be both used as MDNS and Chen et al. used MRI to investigate the in vivo degradation of a cellulose nanocrystal/SF-blended hydrogel [57]. Three month real-time dynamic degradation of the hydrogel was studied using proton-density-weighted imaging as well as T2 and T2* mapping.

Most MRI studies to date have focused on tracing the fate of intact NCs rather than of MDNS released from them. This is probably because of the limitations of MRI as a bioanalytical tool. First, the specificity of MRI is unreliable because the biological matrix can cause strong background noise and interfere with the detection of analytes [39]. Secondly, it is unable to reveal metabolic changes because it is not structurally specific. Thirdly, the accuracy and reproducibility of MRI are limited by inadequate calibration and validation criteria [58]. Finally, contrast agents are likely to alter the in vivo fate of MDNS and are not without some toxicity.

2.4. GPC-RI

GPC-RI is mainly used in the determination of saccharides but it has also received limited application in the bioassay of other MDNS. Grindel et al. have studied the PK of poloxamer 188 in rat, rabbit, dog and man with GPC-RI [59]. Plasma samples were prepared by protein precipitation with acetonitrile and sodium chloride prior to GPC-RI analysis. The analytical method was fully validated and the results demonstrated the method was adequate to study the PK of poloxamer 188 despite its limited sensitivity.

Mohammad et al. used GPC-RI to investigate the degradation of PLGA nanoparticles in tissues following i.v. administration to mice [60]. PLGA was extracted from tissue samples using chloroform after which the chloroform solution was frozen and lyophilized prior to analysis. The application of GPC-RI is again limited due to matrix interference, low sensitivity and poor reproducibility. In addition, GPC-RI is sensitive to temperature and the nature of the mobile phase which may decrease the reproducibility of the technique.

2.5. ICP-MS

ICP-MS is commonly used to determine metals with good selectivity, high sensitivity and multi-isotope detection capability. The MS feature can take a number of forms of which ICP-Q-MS is the most common technique for NP analysis due to its fast data acquisition speed (< 0.5 ms) [61]. Lee et al. used it to investigate the distribution of AgNPs in rat [62] where tissue samples were digested in nitric acid and hydrogen peroxide and diluted with deionized water before silver was determined by ICP-MS. Salimi et al. investigated the biodistribution of FeONPs in tumor-bearing BALB/c mice using a similar method [63] where blood and tissue samples were digested in nitric acid and hydrogen peroxide, diluted with 2% nitric acid before iron was determined by ICP-MS.

In spite of numerous merits and extensive application to studies of metallic NCs, ICP-MS has several limitations. First, it cannot differentiate metal in a DDS or MDNS from endogenous metal. Secondly, it does not provide information about the release or metabolism of MDNS. Thirdly, the sample preparation procedure for ICP-MS is often complicated and time-consuming.

2.6. LC-MS/MS

Because of the excellent selectivity, sensitivity and accuracy, LC-MS/MS is considered the “gold standard” technique for carrying out PK studies of small molecules. However, problems arise when applied to the quantitation of polymeric MDNS due to the fact they are generally polydisperse (i.e. exist as mixtures of polymers with MWs distributed about a central average value) and form multiple product ions during MS/MS detection. Recently, new MS techniques have overcome this problem. Gong et al. quantified PEGs and PEGylated proteins in animal tissue using an in-source collision induced dissociation (CID) strategy [64] (Fig. 6, I). In this technique, PEGs PEGs or PEGylated proteins are fragmented in-source by the declustering potential to produce specific fragments that can be selected as parent ions in Q1. After being transferred to Q2, parent ions are dissociated by the collision energy to generate daughter ions, some of which are selected and transported to the detector via Q3. The LLOQ of the method for 40 kDa PEG was 50 ng/mL.

In contemporaneous studies, Zhou et al. used an MS^{ALL}-based approach with LC-TOF-MS to determine linear PEGs in rat plasma [65] (Fig. 6, II) while Gu and co-workers used the approach to study the fate of PEGylated doxorubicin and paclitaxel after i.v. injection to rats [66,67]. In this approach, no ion is selected in Q1 and all ions are dissociated by the collision energy in Q2 before specific fragments are detected by TOF MS. Compared with the in-source fragmentation strategy, MS^{ALL} provides better selectivity and sensitivity because the collision energy in Q2 provides better dissociation capacity and TOF-MS provides higher resolution.

Current LC-MS/MS technologies are restricted to the bioanalysis of a small number of organic MDNS and need to be further developed. Moreover, LC-MS is not as visual as fluorescence labeling, radiolabeling or MRI since it cannot intuitively reflect the distribution process of MDNS. Nevertheless, LC-MS is a powerful tool for application to metabolism studies.

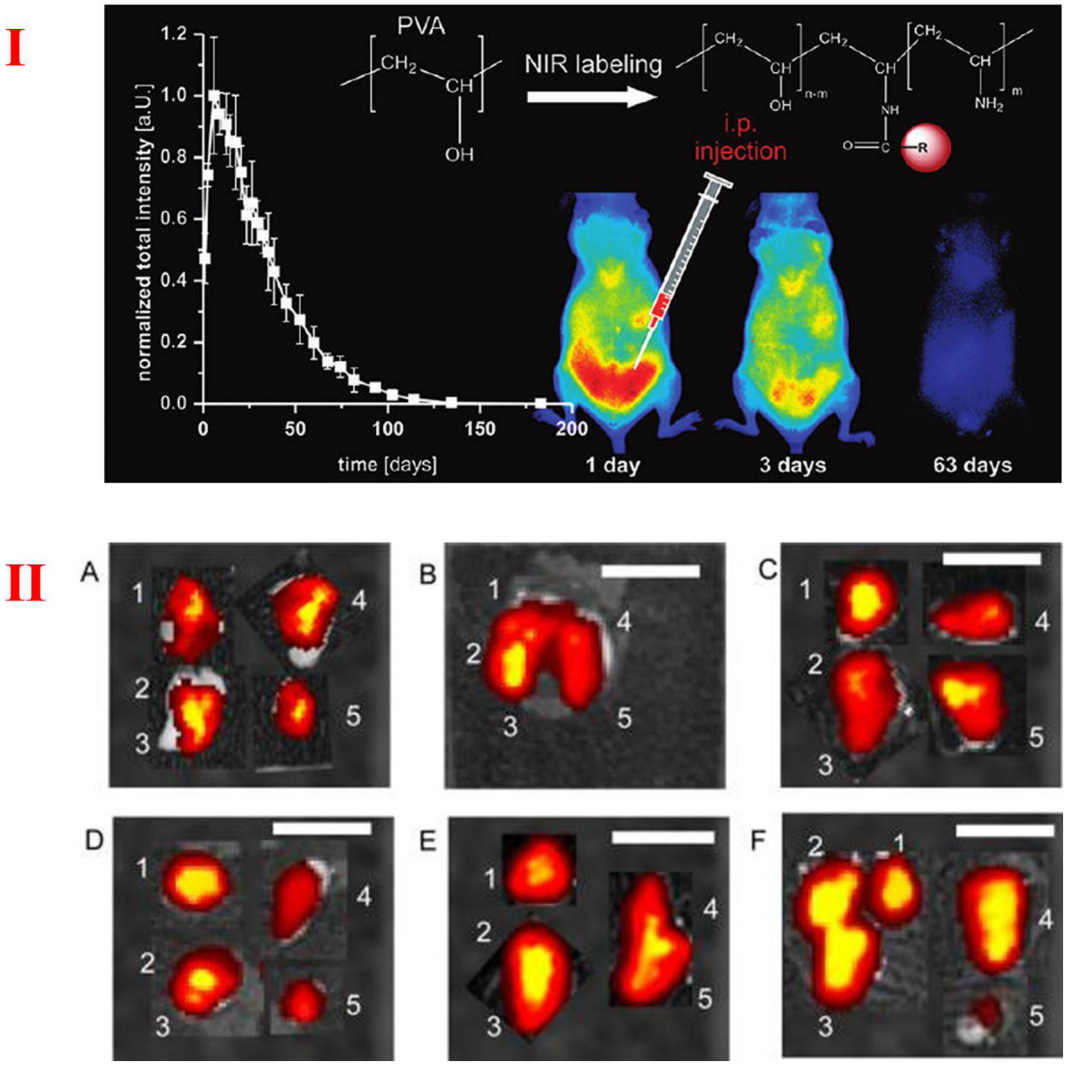

Fig. 4. I: Biodistribution study of 195 kDa PVA in mouse using fluorescence labeling [40]. **II:** Monitoring HA with different molecular weights in lung at different times. [41] Fig. 4 I is reproduced with the permission of the publisher and A. Schädlich et al., *Noninvasive* in vivo *monitoring of the biofate of 195 kDa poly(vinyl alcohol) by multispectral fluorescence imaging*, Biomacromolecules 12 (2011) 3674–3683. Copyright © 2011 American Chemical Society. Fig. 4 II is reproduced with the permission of the publisher and C. Kuehl et al., *Hyaluronic acid molecular weight determines lung clearance and iodistribution after instillation*, Mol. Pharm. 13 (2016) 1904–1914. Copyright © 2016 American Chemical Society.

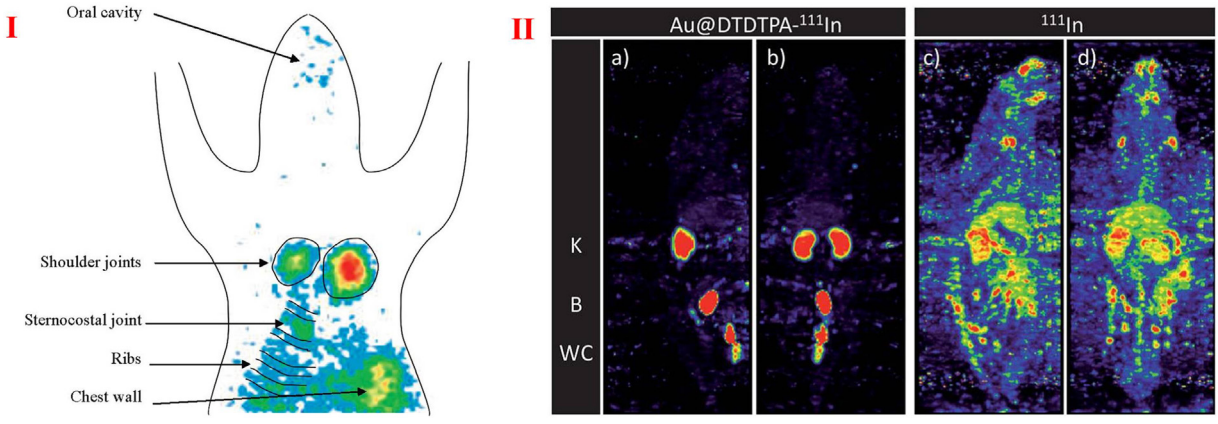

Fig. 5. I: Radioactivity image of ^{99m}Tc-hyaluronan biodistribution in rat. [48]. **II:** Radioactivity image of AuNPs-^{111}In biodistribution in rat. [49] Fig. 5 I is reproduced with the permission of the publisher and L. Balogh et al., *Absorption, uptake and tissue affinity of high-molecular-weight hyaluronan after oral administration in rats and dogs*, J. Agric. Food Chem. 56 (2008) 10582–10,593. Copyright © 2008 American Chemical Society. Fig. 5 II is reproduced with the permission of the publisher and C. Alric et al., *The biodistribution of gold nanoparticles designed for renal clearance*, Nanoscale 5 (2013) 5930–5939. Copyright © Royal Society of Chemistry 2013. [B: bladder; K: kidney; WC: urine collection tube; Au@DTDTPA: nanoparticles made up of a gold core and a dithiolated polyaminocarboxylate shell].

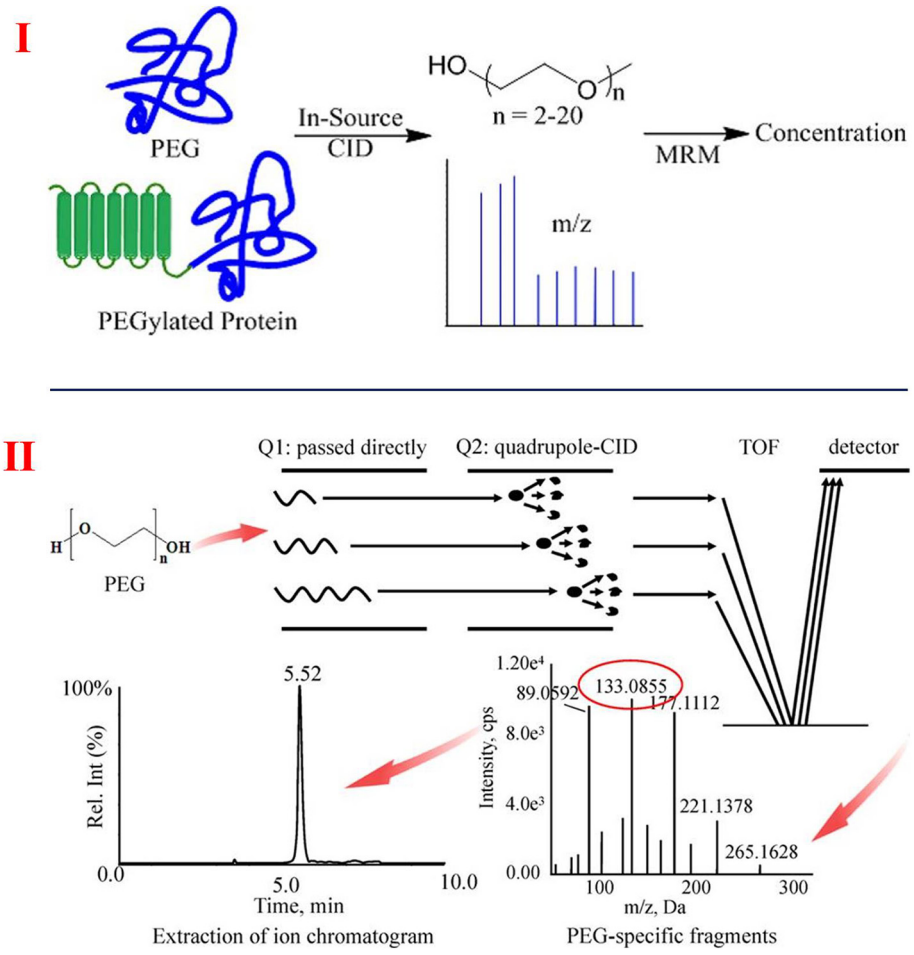

Fig. 6. I: In-source collision induced dissociation (CID) strategy for the determination of PEG and PEGylated protein by LC-MS. [58] **II:** MS^{ALL} strategy for the determination of PEG by LC-MS. [59] Fig. 6 I is reproduced with permission from the publisher and J. Gong et al., *Quantitative analysis of polyethylene glycol (PEG) and PEGylated proteins in animal tissues by LC-MS/MS coupled with in-source CID*, Anal. Chem. 86 (2014) 7642–7649. Copyright © 2014 American Chemical Society. Fig. 6 II is reproduced with permission from the publisher and X. Zhou et al., *Development and Application of an MS(ALL)-Based Approach for the Quantitative Analysis of Linear Polyethylene Glycols in Rat Plasma by Liquid Chromatography Triple-Quadrupole/Time-of-Flight Mass Spectrometry*, Anal. Chem. 89 (2017) 5193–5200. Copyright © 2017 American Chemical Society. (CID: collision induced dissociation)

3. ADME of NCs

3.1. Absorption

Absorption of an NC into the blood subsequent to administration by the oral, inhaled or dermal routes involves two processes viz. interaction with the internal environment of the organism and passing through a bio-barrier [68–70]. In this case, NCs are transported to regional lymph nodes before distribution into blood [71]. These administration routes can provide slow release of drug so that less frequent administration is possible. In contrast, i.v. administration of an NC brings it into immediate contact with the blood where it may undergo aggregation due to the high ionic strength [72]. This can lead to obstruction of blood capillaries and, in the case of larger NPs, formation of an embolism [1].

NCs ingested orally may penetrate epithelial barriers either directly by passive transcellular or paracellular diffusion or indirectly as a result of carrier-mediated cellular uptake followed by transcytosis [73]. NCs ingested via inhalation into the lung may cross the pulmonary barrier and undergo capture and clearance in the pulmonary microenvironment [70]. NCs applied to the skin must cross the epidermis and dermis, and stratum corneum, the most superficial layer of the epidermis, is the main obstacle to the process of absorption. Generally, only small NCs can penetrate the stratum corneum [70,74].

Following administration of an NC, MDNS can be produced at any stage of NC distribution and undergo one or more stages of ADME in their own right. ADME studies of MDNS reveal their potential impact on the organism and are important to understand their potential toxicity and to guide the design of safer NCs [70].

3.2. Distribution

After absorption, NCs are distributed throughout the body and dispersed in tissues where they may accumulate if administered over a prolonged period. The size, shape and surface properties of NCs can be fine-tuned in order to prolong blood circulation and enhance targeting to a particular site [70]. However, NCs in the bloodstream are apt to adsorb plasma components which can change their charge and size and thereby alter their physicochemical properties [75]. In addition, the adsorption of plasma proteins onto an NC can make it be recognized by the mononuclear phagocytic system (MPS) and its subsequent clearance from the circulation [76].

Although general rules for the biodistribution of NCs have yet to be developed, it is clear that certain factors can influence the process [50]. First, smaller NCs undergo better distribution to tissues than their larger counterparts partly because those with size >200 nm are generally eliminated by the spleen [77,78]. Secondly, in cancer treatment, NCs with size in the range 10–200 nm tend to distribute to tumor tissue at high concentration in virtue of the EPR effect [79]. Thirdly, a non-spherical rather than a spherical shape appears to increase circulation time and promote accumulation [80].

Functional modification of NCs can improve their targeting ability. Folic acid is an extensively used ligand for targeting the membrane of

cancer cells and enhancing NC endocytosis via the folate receptor which is commonly overexpressed by cancer cells [81]. Anisamide achieves the same goal by interacting with overexpressed sigma receptors on tumor cells [82–85]. Glycyrrhetinic acid and galactose are widely used to enhance distribution of NCs to the liver [86,87]. Modification with peptides, proteins, nucleic acids and nucleic biotin can also improve the targeting of a DDS [79].

3.3. Metabolism

The metabolism of NCs mainly depends on the route of absorption and their surface characteristics [76]. NCs can be cleared from the body via structural degradation and excretion in non-degradable form [88]. In the case of inorganic NCs, they are generally considered to be resistant to degradation and metabolism and display long residence times in the body [71]. For example, PEGylated quantum dots can remain in the body for at least two years [89]. However, some researchers disagree with this point of view as has been discussed elsewhere [90,91]. Because of the acidic environment in lysosomes, degradation of inorganic NCs can release metal ions that can subsequently bind to different biomolecules [92]. Moreover, chemical groups on the surface of inorganic NCs can be metabolized enzymatically or non-enzymatically.

In the case of organic NCs (those made up of organic MDNS), enzymatic degradation depends on their chemical composition and physicochemical properties [1]. Organic NCs are likely to first dissociate to MDNS which are then metabolized to smaller components [1,93]. Yin et al. and Sun et al. detected PEGs dissociated from polymeric NCs in vivo [66,67]. In the liver, MDNS too large to pass through transcellular pores between liver sinusoidal endothelial cells can be filtered whereas small MDNS can traverse the pores, access the Disse space and then enter hepatocytes [70,94]. MDNS may then experience enzymatic metabolism [95,96] by enzymes such as mono-oxygenases, transferases, esterases and epoxide hydrolase [70]. The metabolites produced are either excreted in urine or transported to the bile and ultimately excreted in the feces. Overall NCs may produce a wide range of metabolites differing in size, shape and chemical form [70].

3.4. Excretion

Excretion is an essential process that serves to reduce the potential toxicity of NCs. Excretion by renal clearance takes place via glomerular filtration which depends on the shape, size and charge of the NC [97,98]. In general, particles with diameter < 6 nm can traverse glomeruli, enter the bladder and undergo elimination in the urine. However, surface charge influences the excretion of particles with diameter 6–8 nm since crossing glomeruli is easier for positively charged particles [70,99]. After traversing the glomerular capillaries and entering the Bowman's space, some particles undergo tubular reabsorption and return to the blood. Particles that are not reabsorbed traverse the glomeruli and are excreted in the urine [70]. It has been reported that a number of polymer-based NCs are excreted in the urine [70,100].

For non-biodegradable NCs with diameter > 6 nm, excretion is exclusively into bile. Compounds with low MW are handled by active transport [101] whereas those with higher MW undergo paracellular and transcellular transport [102]. For example, 50 nm polystyrene NCs are primarily eliminated in bile as intact particles [103]. However, as started above. Charge on NCs influences the process of biliary excretion [104,105].

4. ADME of MDNS

4.1. Polyesters

PLA, PLGA and PCL are polyesters commonly used in the preparation of NCs. PLA is a linear, aliphatic polyester made up of L, D or racemic forms [106] which have different mechanical properties and degradation profiles [107]. PLA is biocompatible [108], and FDA has ratified its application in medicines and medical devices [109]. Despite its widespread use in NCs [109], the ADME of PLA MDNS have received little attention.

The European Medicines Agency (EMA) and FDA have authorized the application of PLGA copolymers in drugs and medical devices because they are biocompatible, relatively non-toxic and able to control drug release [110,111]. PCL is a semi-crystalline polymer which has been authorized by the FDA for clinical application in NCs [112]. Its hydrophobicity enhances its cellular uptake [113] and extends its half-life in vivo promoting its use for sustained delivery of encapsulated peptides and proteins and their protection from acidic degradation [112].

4.1.1. Absorption

At the present time, there is no information relating to the absorption of PLA and only one study relating to that of PCL. The latter investigated subcutaneous (s.c.) implantation of PCL capsules in rats [114] and showed that PCL can be slowly absorbed into the blood. In fact, PCL was only detected in plasma 15 days after implantation, did not reach its highest level until after 45 days and required 165 days before it was completely cleared from the system.

There is also little information relating to PLGA absorption but a study of the ADME of PLGA-NPs has been carried out [115]. It showed they are absorbed after oral administration but no details were provided. After topical administration of PLGA-NPs to the skin, Wei et al. [115] showed that the stratum corneum is the main barrier to absorption although some occured by passive permeation via the follicular pathway. Greater absorption resulted from breaking the stratum corneum using microneedles which facilitated the passage of NCs through both the epidermis and dermis.

4.1.2. Distribution

After PCL was administered to rat by s.c. injection, it was not detected in organs presumably because of its slow rate of absorption [114]. There are no studies describing the distribution of PLA possibly because of its rapid degradation by ester hydrolysis. As stated above, Wei et al. studied the fate of topically administered PLGA NPs through human skin treated with microneedles [115]. They found that the NPs preferred to distribute into the epidermis compared with the dermis and the distribution was size-dependent and increased with NP concentration up to a limiting value. In a study by Navarro et al. involving oral administration of PLGA NPs to F344 rats, the concentration was highest in spleen followed by kidney, intestine, liver, lung, brain and heart [116]. However, in another study involving similar administration to Balb/C mice, Semete et al. found the concentration was highest in liver followed by kidney, brain, heart, lung and spleen [117]. The authors speculated the difference was not only due to the different animal species but also to differences in size, shape and surface characteristics of the NPs used in the two studies. In particular, the NPs used by Navarro et al. were 200–350 nm in size and hence were cleared by the spleen [77,78] leading to the high spleen concentration found, whereas the NPs used by Semete et al. were smaller (112 ± 9 nm) and were probably cleared mainly by the liver.

Park et al. investigated the biodistribution of PLGA NPs in mice hepatocytes after injection into the spleen [118]. The authors found that only 7% of hepatocytes took up the NPs with Kupffer cells taking up most [118]. It has also been reported that grafted PLGA scaffolds in the body often result in inflammation around implants [16]. This finding raises questions about the safety of drug-loaded PLGA NPs.

4.1.3. Metabolism

PLA can be degraded by ester hydrolysis to produce lactic acid [119,120], an endogenous substance generated by muscles [121] which subsequently enters the Krebs cycle to be metabolized to H_2O and CO_2. PLA hydrolysis in vivo is a heterogeneous reaction involving diffusion control and autocatalysis [119]. Ester bonds are first

hydrolyzed to produce oligomers that can diffuse to surface and undergo complete hydrolysis. Autocatalysis is triggered by PLA oligomers that remain inside the matrix [119]. Because lactic acid is an endogenous substance, it is generally considered safe but it can decrease the pH of the surroundings and cause inflammatory tissue reactions [122]. In fact, chronic inflammation as indicated by the presence of macrophages, fibroblasts, giant cells and lymphocytes has been observed in dogs after meniscal reconstruction with poly-L-lactide based materials [123]. Moreover, Taylor et al. proved that accumulation of lactic acid in water incubation solutions can lead to toxicity [124].

PLGA undergoes hydrolysis to produce lactic acid and glycolic acid, and either of them can get into the Krebs cycle and be degraded to H_2O and CO_2 [110,125]. Polymer degradation can be influenced by intrinsic properties and environmental parameters. Generally, degradation is more rapid for amorphous polymers with low MW, good hydrophilicity and high glycolide content [125]. Mohammad and Reineke studied degradation of PLGA NPs in tissues after i.v. administration [60] and found that breakdown was greatest in the liver due to its high concentration of esterases [60]. The in vivo degradation of PCL in rat was also mediated by esterases but details of the process were not provided [114].

4.1.4. Excretion

Only one report describing the excretion of PCL has been published which showed that >90% is excreted in feces and urine after s.c. injection in rat [114]. Studies of the excretion of PLA and PLGA have not been reported probably because they are efficiently degraded in vivo to multiple products that pose a big challenge to analytical methods.

4.2. PEGs and PEG-associated derivatives

PEGs are hydrophilic and neutral polymers made up of ethylene oxide units that exist as both branched and linear forms. They are stable, innoxious and biocompatible and as a result have been authorized by the FDA for clinical use by parenteral administration [126,127]. Low MW PEGs are often used to regulate the solubility and viscosity of drug carriers whereas high MW PEGs are mainly used as structural material to regulate drug release from DDS. They are commonly used in NCs to reduce their immunogenicity and antigenicity, increase their water solubility and extend the circulation half-life of the payload drug [65].

Poloxamer is a copolymer made up of various lengths of ethylene oxide (EO) and propylene oxide (PO) [23] in the form of a triblock copolymer EO_a-PO_b-EO_a [128]. Different poloxamers are named with the letter "P" (for poloxamer) followed by three digits, the first two multiplied by 300 giving the approximate PO MW and the third multiplied by 10 giving the percent of EO (e.g. P188 has a PO MW of 5400 Da and an EO content of 80%) [23]. When used in NCs, poloxamers can promote uptake by cancer cells, increase drug cytotoxicity [129] and enhance drug stability [130]. Currently, ADME information is only available for P188.

4.2.1. Absorption

Absorption of PEGs from the GI tract is MW dependent, decreasing as MW increases. For example, it was found that only 2% of PEG 1000 was absorbed from the GI tract of rats and PEGs with MW in the range 4000–6000 Da were not absorbed even after 5 h [131]. In humans, oral absorption decreased from 57% for PEG 500 to 9.8% for PEG 1000 to virtually zero for PEG 6000 [132]. After oral administration of 17 g PEG 3350 to healthy individuals, only 29 mg was absorbed into the blood, the rest being excreted in the feces [133]. This poor bioavailability may result from the tendency of PEGs to absorb water and thereby increase their volume. As for transdermal administration, PEGs with MW < 4000 are absorbed to only a small extent through intact skin, and PEGs with higher MW are not absorbed at all [134].

4.2.2. Distribution

Knop et al. found that PEGs administered by i.v. injection to mice could be detected in kidney, lung, heart, liver, GI tract, spleen and gall bladder [8]. In a study by Rudmann et al. [135], PEGs of various MW (10, 20 and 40 kDa) administered as an i.v. 100 mg/kg injection were still detected in kidney, spleen, liver, lungs, heart and choroid plexus after three months. Concentrations were highest in choroid plexus and spleen for PEG 40000 and in lungs and kidney for PEG 10000.

In a study of the distribution of PEGs in mice after i.v. administration, Yamaoka et al. [136] found highest concentrations in liver and GI tract. The accumulation of high MW PEGs in liver is of concern since it has the potential to cause macromolecular syndrome [137]. PEG MW has little influence on the distribution profile but clearance from tissues/organs decreases with increasing MW. Accumulation is time-dependent on account of the vascular permeability. Thus low MW PEGs freely distribute between blood and extravascular tissues by diffusion whereas high MW PEGs translocate more slowly [136]. This means that chronic administration of large doses of high MW PEGs can cause serious accumulation in organs and lead to potential toxicity.

Some researchers have studied the distribution of PEGs released from NCs in vivo. Yin et al. investigated the distribution of PEG 2000 released from PEGylated doxorubicin administrated by i.v. injection to tumor-bearing mice [138]. They found that released PEG distributes mainly to kidney followed by liver and remained detectable up to 46 h. Sun et al. carried out a similar study after i.v. injection of PEGylated paclitaxel [139] and found PEG 2000 distributed mainly to kidney and bladder in the first hour and to spleen and liver after 12 h.

Grindel et al. investigated the tissue distribution of P188 after i.v. injection to dogs and rats [49]. After 48 h, P188 was widely distributed throughout the body but was high concentrated in kidney with the potential to cause dose-dependent renal dysfunction characterized by coarse vacuolization of the proximal tubule epithelium. [23]

4.2.3. Metabolism

Webster et al. reviewed the metabolism of PEGs [14] and concluded it occurred mainly by oxidation of the terminal alcohol group to a carboxyl acid [15]. Both hydroxyacid and diacid metabolites were found in burn patients, cats and rabbits. Sulfated PEG metabolites have also been observed in rat and guinea pig liver. In mammalian systems, the oxidation is mainly mediated by alcohol dehydrogenase, with CYP450s and sulfotransferases playing a lesser role. Although toxicological studies indicate the metabolites are non-toxic, the acid metabolites are thought to be responsible for the acidosis and hypercalcemia observed in patients taking overdoses of PEGs.

The extent of PEG oxidation appears to decrease as MW increases with some 25% of PEG 400 being metabolized in both human and rabbit but only 15% of PEG 1000 being metabolized in human and only 4% of PEG 6000 in rabbit. A similar situation exists for sulfation where PEG 200 is extensively metabolized in rat and guinea pig but PEG 6000 is not sulfated at all.

Grindel et al. found a single metabolite of P188 in dog, rat and human [49,59]. The metabolite had a MW of approximately 16,000 Da and produced MALDI-MS fragmentation consistent with a block copolymer. The authors concluded it was a high MW fragment of P188 [49] that was cleared more slowly than P188 itself [59].

4.2.4. Excretion

Excretion of PEGs is also MW dependent. Low MW PEGs mainly undergo renal clearance by passive glomerular filtration whereas those with high MW are mainly excreted into bile [14,140]. In mouse, urinary excretion was markedly less for MW > 20,000 Da [136], and in dogs the plasma elimination rate of PEGs with MW in the range 400–4000 Da was consistent with glomerular filtration [141]. In mass balance studies after i.v. injection in human, 86% of PEG 1000 and 96% of PEG 6000 were eliminated via the kidney over 12 h [142] compared with 100% of PEG 1000 in rat [140].

The MW threshold for kidney clearance of PEGs does not apply to proteins because other factors influence the filtration process [137]. For instance, PEGs can absorb more water molecules than proteins of the same MW resulting in a bigger hydrodynamic volume and a lower MW threshold for biliary clearance. However, the linear and flexible nature of PEGs allows them to cross glomerular membranes by 'snake-like' movements. The glomerular filtration threshold for PEGs has been calculated to be 30 kDa [137] but other studies show that PEGs with MW as high as 190 kDa are excreted by glomerular filtration [136].

For high MW PEGs, biliary excretion is the main elimination pathway and is also MW-dependent. In mouse, biliary excretion is minimal for PEGs with MW about 50 kDa and is higher for PEGs with both lower and higher MW [136] possibly because the uptake of PEGs by Kupffer cells increases as MW increases above 50 kDa [136]. Schaffer et al. reported that PEG 400 administered by i.v. injection is not eliminated by biliary excretion in bile duct-cannulated dogs [142]. For PEG 900, Friman et al. suggested that biliary clearance was a passive process [143] whereas Roma et al. speculated that vesicular transport via the lysosome was an active component of biliary excretion [144].

In separate studies, Yin and Sun investigated the release of PEG 2000 from PEGylated drugs [138,139]. After i.v. injection of 1 mg/kg PEGylated doxorubicin to tumor-bearing mice, 42.7% of PEG 2000 was excreted in urine and only 0.298% in feces. Similarly, after i.v. injection of 25.8 mg/kg PEGylated paclitaxel (PEG 2000) to rats, 44.0% of PEG 2000 was excreted in urine and 2.02% in feces. For P188, renal clearance is the main route of elimination in human accounting for about 90% of total body clearance after i.v. injection [51]. Fecal excretion accounted for only about 0.025% of the dose over 96 h [49].

4.3. Polysaccharides

Chitosan and HA are common polysaccharides used in preparing NCs. Chitosan is a linear aminopolysaccharide which, like cellulose, consists of D-glucosamine and *N*-acetyl-D-glucosamine [145]. Under alkaline conditions, chitosan can be produced by deacetylation of chitin [146]. Chitosan is a nontoxic, biodegradable polymer of low immunogenicity [147,148] which is approved in Japan, Italy and Finland for dietary applications [149] and by the FDA for use as a wound dressing [150]. Because of its cationic nature and mucosal adhesiveness, it has been widely used in a variety of DDS [151]. For example, chitosan nanoparticles are extensively used due to their unique ability to target organs and tumors [152–154].

HA is a natural mucopolysaccharide made up of D-glucuronic acid and *N*-acetyl-D-glucosamine with a MW > 1000 kDa [155]. It is ubiquitously present in almost all vertebrate tissues and participates in many cellular processes [50]. Due to its biocompatibility, non-immunogenicity and unique viscoelastic and lubricating properties, HA has been applied in various medical devices. It has also facilitated the development of NCs that actively target drugs and genes to tumor cells. Such NCs are produced by chemical conjugation of HA to preformed lipid-based NCs and polymeric NPs or as self-assembling NCs that use chemically modified HA as the backbone [156–158]. The selective toxicity of HA-based NCs results from the overexpression of HA receptors on cancer cells [159].

4.3.1. Absorption

Onishi et al. reported that FITC-labeled chitosan and carboxymethylchitosan are rapidly and efficiently absorbed after i.p. administration [160]. Kato et al. observed that absorption of highly succinylated N-succinylchitosan into blood after i.p. administration took several hours but reached an efficiency of 87% [161]. Later research by Dong et al. showed absorption of carboxymethylchitosan after i.p. administration was MW dependent [42]. Furthermore, Chae et al. reported that FITC-labeled chitosans with MW 3.8 kDa achieved high plasma concentrations after oral administration whereas those with MW 230 kDa showed virtually no absorption [162]. Orally administered oligomers are absorbed to a small extent but larger MW chitosans are directly excreted with no absorption [163]. It has been speculated that lower MW carboxymethylchitosans and their degradation products are more easily transported from the blood to peripheral tissues than higher MW ones [161] suggesting low MW derivatives are preferable for preparing NCs to be administered extravascularly.

Another important property of chitosan is its positive charge at low pH. This results in the formation of salts with negatively charged fatty acids and bile acids in the stomach and GI tract that can reduce their absorption. Being hydrophobic, chitosan can also bind to lipids (e.g. cholesterol and other sterols) to reduce their emulsification [21]. It has also been reported that chitosan can promote platelet adhesion [22]. These properties suggest further research is needed into the clinical use of chitosan based NCs.

In relation to HA, Oe et al. reported that about 90% of ^{14}C-labeled HA is absorbed by the GI tract to be utilized as energy or structure composition of the body [164]. Absorption has been shown to take place in the large intestine [165]. Interestingly, Laznicek et al. found that ^{99m}Tc-labeled HA was not absorbed in rats after oral administration [50] which presumably results from the different radioisotopic label [165].

4.3.2. Distribution

After i.v. administration to rats, Richardson et al. found that chitosans with high MW accumulate in the liver to a potentially toxic level [166]. Similar results were found by other researchers [167–169] who also observed accumulation in the stomach [170,171]. After i.v. administration to mice, chitosan N-octyl-O-sulphate distributes mainly to the kidney [171]. After i.p. administration to mice, FITC-labeled chitosan also distributes mainly to the kidney [160] whereas FITC-labeled carboxymethylchitosan was found in the liver, spleen and kidney [148]. In fact, biodistribution of chitosan in mice is similar after i.p. and i.v. administration [163]. In rats, ^{125}I-labeled chitosan distributes primarily to liver but at low concentrations 2 days after injection into the hepatic artery it is found mainly in stomach and muscle [54].

After i.v. administration of ^{99m}Tc-labeled HA, Laznicek et al. found the highest level of radioactivity in the liver with some in the kidney due to elimination of HA fragments [50]. After i.v injection, Courel et al. [172] found the highest level of tritiated HA in kidney, spleen and liver with some in bone marrow of mice. After oral administration, radioactivity was only detected in the GI tract [50].

In contrast, Oe et al. studied the distribution of ^{14}C-labeled HA and found high radioactivity in intestine, pancreas, harderian gland, liver, and mandibular gland after oral administration [164]. Balogh et al. found that after oral administration of ^{99}Tc-labeled HA to rats and dogs, radioactivity was found in blood, skin, joints, bone and muscle [51]. Again these differences are probably the result of the different radioisotopic labels. Kimura et al. demonstrated that the migration of HA to the skin is via the blood or lymph [165]. After pulmonary administration via intratracheal instillation in mice, the highest HA levels were found in the lung followed by the GI tract [43] (Fig. 7, I).

4.3.3. Metabolism

Enzymes can degrade chitosan by hydrolyzing bonds between glucosamines, *N*-acetylglucosamines and each other. In vertebrates, chitosan is mainly degraded by muramidase and enzymes produced by bacteria in the GI tract [163]. Three chitinases of human viz. chitotriosidase, acidic mammalian chitinase and di-*N*-acetylchitobiase were shown to have hydrolytic activity [173]. Possible sites of chitosan degradation after i.v. administration are thought to be the liver and kidney, the former playing a central role in degradation after i.p. administration [163,174]. It has also been reported that chitosan administered by i.p. injection is degraded in the peritoneal cavity [148].

After oral administration, chitosan breakdown occurs principally in the gut in a species-dependent manner. Thus, breakdown is more extensive in hens and broilers than in rabbits. Interestingly, N-stearoylchitosan breakdown is insignificant demonstrating that

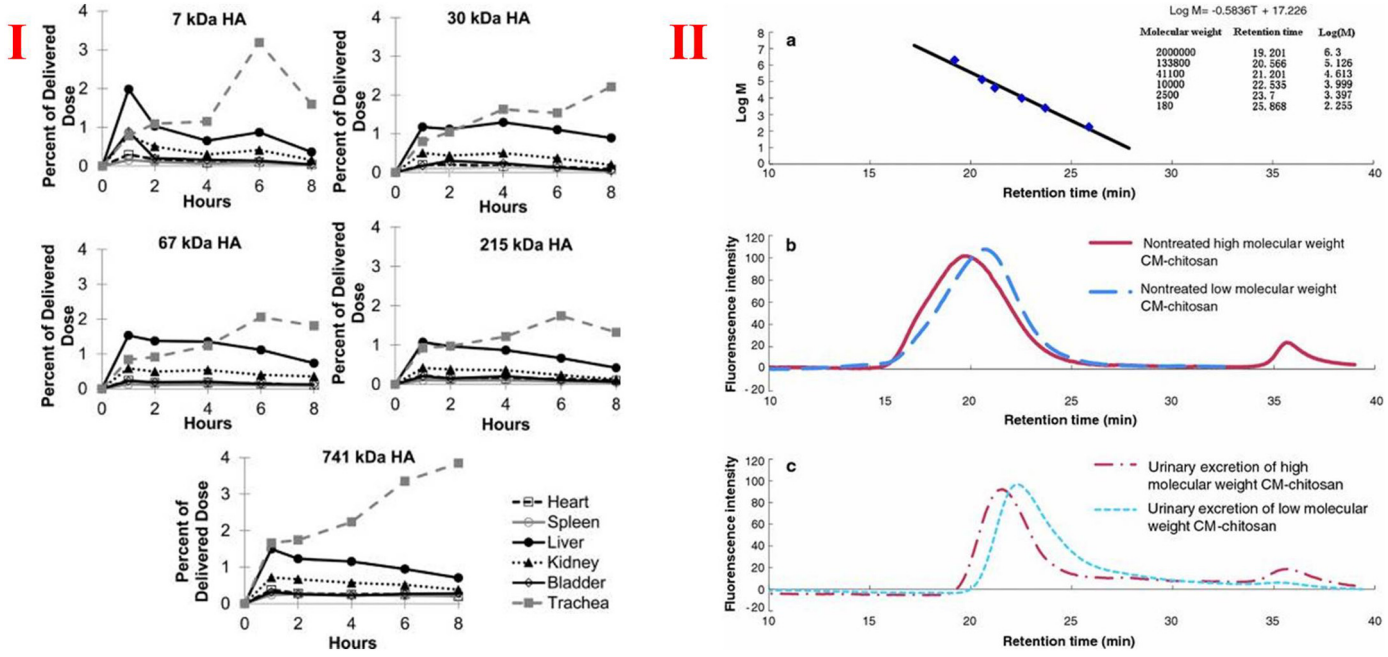

Fig. 7. I: Distribution degrees of HA with different molecular weight in different organs. [41] **II:** (a) Dextran standard curve; (b) GPC curve of non-treated carboxymethylchitosan; (c) GPC curve of urinary excreted carboxymethylchitosan degradation products at 6 h after intraperitoneal administration. [160] Fig. 7 I is reproduced with permission from the publisher and C. Kuehl et al., *Hyaluronic acid molecular weight determines lung clearance and biodistribution after instillation*, Mol. Pharm. 13 (2016) 1904–1914. Copyright © 2016 American Chemical Society. Fig. 7 II is reproduced with permission from the publisher and W. Dong et al., *Effects of molecular weights on the absorption, distribution and urinary excretion of intraperitoneally administrated carboxymethyl chitosan in rats*, J. Mater. Sci. Mater. Med. 23 (2012) 2945–2952. Copyright © Springer Science+Business Media, LLC 2012. (CM-chitosan: carboxymethyl chitosan; HA: hyaluronic acid)

enzymolysis of chitosan relies on the presence of free NH_2 groups. Furthermore, the chitosan degradation speed depends on MW and degree of acetylation [163]. Low MW degradation products can be subsequently channeled into the biosynthesis of structural components such as glycoproteins [42].

Administered HA is first phagocytized by liver endothelial cells and then transported to lysosomes for disposal [50]. Hyaluronidases, six of which have been identified to date, can hydrolyze linkages between *N*-acetyl-D-glucosamine and D-glucuronic acid [175] after which further degradation leads ultimately to CO_2, H_2O and urea [44]. There are two kinds of human hyaluronidase, one of which, hyaluronidase 2, metabolizes HA into 20 kDa subunits and the other, hyaluronidase 1, metabolizes HA in the blood to tetrasaccharides. These tetrasaccharides are then broken down to monosaccharides by glucosidase in the liver and utilized as an energy source before being ultimately expired as carbon dioxide [165]. Interestingly, not all internalized HA is metabolized within lysosomes since some is sequestered into vesicles of various sizes [176]. It has also been reported that HA can be fragmented by oxygen radicals in tissues [177] and degraded to oligosaccharides by bacteria in the cecum [165].

4.3.4. Excretion

Suzuki et al. reported that, after i.v. administration of holmium-166 labeled chitosan to rats and mice, 4–5% of chitosan was recovered in feces and urine and about 90% in the corpse [178]. After i.p. administration of FITC-labeled chitosan and carboxymethylchitosan to rats, urinary excretion was the major route of elimination [148,160] (Fig. 7, II). Investigation of its dependence on MW showed 88% of high MW FITC-carboxymethylchitosan was excreted over 15 days compared with about 71% of low MW FITC-carboxymethylchitosan [42].

Oe et al. reported that after oral administration of ^{14}C-labeled HA to rats, 3.0% of the radioactivity was excreted in urine, 11.9% in feces and 76.5% in expired air [164]. Balogh et al. did the same experiment using ^{99m}Tc-labeled HA and found that about 90% of the radioactivity was excreted in feces and 3% in urine [51]. This difference is presumably the result of using different labeling reagents. After i.v. administration to rats, 70% of ^{14}C-labeled HA was recovered in exhaled breath and 22% in urine compared with 63% and 20% respectively in rabbits [179].

4.4. Polyenes

Currently, polyenes are extensively used in NCs with PVP and PVA being the two most common MDNS. FDA has authorized numerous biomedical applications of PVA because of its biocompatibility, low toxicity and non-immunogenicity [180,181]. PVA is synthesized by first polymerizing vinyl acetate monomer to poly(vinyl acetate) and then hydrolyzing it to produce poly(vinyl alcohol) [182]. PVP is a macromolecular, nonionic polymer with good stability over a wide range of pH that has also been widely used in preparing NCs [183,184]. It acts as a surface stabilizer by reducing NC aggregation due to repulsive forces resulting from its hydrophobic carbon chains [185].

4.4.1. Absorption

Kaneo et al. reported that the rate of PVA absorption into blood from different injection sites decreases in the order i.p. > intramuscular > s.c. [182]. Absorption after i.p. administration involves two main pathways: entering the peritoneal blood microcirculation followed by traversing the liver to drain into the portal vein, and directly traversing the peritoneal lymphatic system to enter the blood [41]. Yamaoka et al. found that PVA absorption rate was shown to be MW dependent [186]. It has also been reported that PVP can be absorbed from the GI tract after oral administration [187] but details of the process were not provided.

4.4.2. Distribution

Wessel et al. reported that i.p. administration of PVP (MW > 30,000) to humans leads to its accumulation in various tissues [188] possibly leading to pulmonary fibrosis, joint pain, and skin sarcoidosis [189]. Other researchers have also observed accumulation in organs and tissues with detrimental effects. Besides ureteral and duodenal blockage [190] these include: in bone marrow and kidney causing pancytopenia and decreased renal function; in nerve tissue, skin, and muscle leading to polyneuropathy, subcutaneous nodules, and pathological fracture

[191]; and in lung causing pulmonary fibrosis [192]. PVP accumulation has also been observed in the ovaries and liver [17,193]. PVP accumulation in tissues increases with increasing MW [17] requiring some caution when selecting it for use in NCs.

Distribution of PVA is also MW-dependent as shown by Yamaoka et al. who administered it to mice by i.v. injection. They reported that accumulation occurred in liver and GI tract and was greater for intermediate MW PVA than for either higher or lower MW material [194]. However, the half-life in blood was found to increase with increasing MW [194]. Kaneo et al. investigated the PK of i.v. administered PVA in rats and mice and found the tissue level was only significant in liver, where PVA can be endocytosed by parenchymal cells, and in spleen [182]. Andreas et al. reported that after i.p. administration of high MW PVA (195 kDa) to mice, PVA accumulated to high levels in fat tissues of the abdomen and kidney, under the skin and to a small extent in the liver [40] (Fig. 8). Overall, it appears that liver is the main site of accumulation leading to the possibility of hepatotoxicity after administration of PVA-based NCs.

4.4.3. Metabolism

In rats and mice, Kaneo et al. proved that intravenously administrated PVA is resistant to metabolism and that no metabolites were found in urine or feces [182]. Similarly it was found to be eliminated unchanged after i.p. administration [41]. Information relating to PVP metabolism has not been reported.

4.4.4. Excretion

Excretion of PVA and PVP is also MW dependent. In rats and mice, intravenously administrated PVA is excreted in both urine and feces with urinary excretion being the main pathway [182]. Low MW PVAs undergo more rapid urinary excretion than high MW PVAs [195] although PVAs with MW and size above the limitation for glomerular filtration (molar mass > 80,000 Da; molecular radius > 4.4 nm) are excreted through the kidney [196]. This phenomenon is due to the flexibility of high MW PVA and its ability to change molecular shape [40]. However, high MW PVA takes a long time to be fully eliminated from the body [41]. PVA taken up by the liver is slowly transferred by the bile duct and gall bladder to the intestinal tract and finally eliminated via feces. Biliary excretion is independent of dose suggesting it does not involve saturable transport processes. PVP is also excreted via both feces and urine after i.v. injection [197–199] with the clearance becoming slower as MW increases [200].

4.5. SF

SF fibers produced by the *Bombyx mori* silkworm have a diameter of 10–25 mm and consist of light chain, heavy chain, and small glycoprotein [201,202]. SF is considered to be biocompatible, biodegradable and of low immunogenicity [202] and as a result has found application in the preparation of NCs. This is because: (a) sensitive protein and nucleic acid therapeutics can be loaded onto SF under mild aqueous

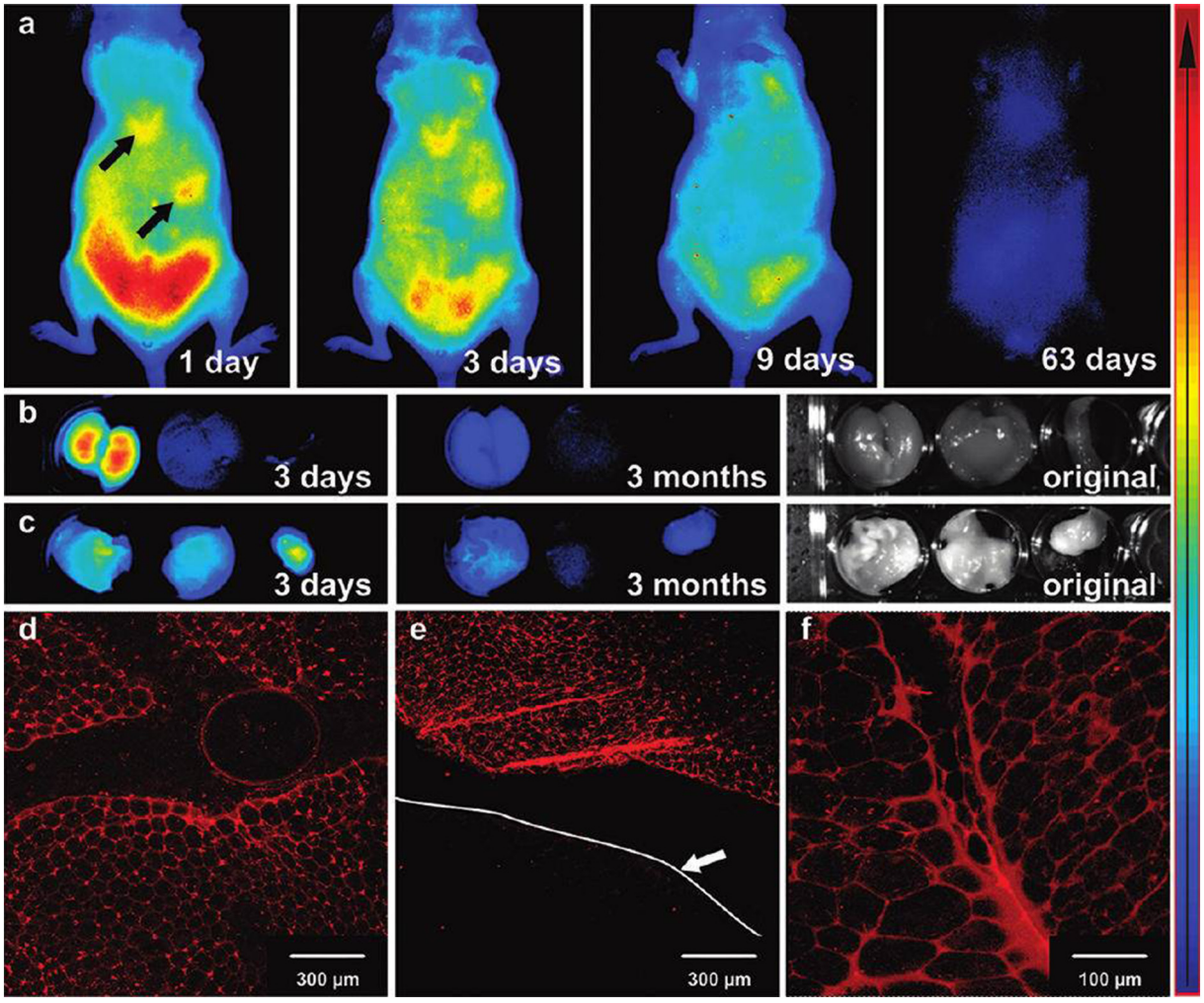

Fig. 8. (a) Fluorescence images of PVA distribution in mouse; (b and c) fluorescence images of PVA distribution in different tissues; (d-f) confocal microscopy images of PVA distribution in fat tissues. [40] Fig. 8 is reproduced with permission from the publisher and A. Schädlich et al., *Noninvasive* in vivo *monitoring of the biofate of 195 kDa poly(vinyl alcohol) by multispectral fluorescence imaging*, Biomacromolecules 12 (2011) 3674–3683. Copyright © 2011 American Chemical Society. [PVA: poly(vinyl alcohol)].

conditions that prevent their dissolution and their thermal and enzymatic degradation [203,204]; (b) loading is facilitated by the fact that SF contains amino acids to which various biomolecules can be attached [205]; and (c) SF can be modified by genetic manipulation to introduce functional domains that can bind to a variety of substances [206]. At the present time, information dealing with the ADME of SF-based NCs is limited probably because SF is unstable in vivo.

Like most proteins, SF can be broken down in vivo into amino acids [207] by proteolytic enzymes such as chymotrypsin, actinase, and carboxylase [202,207]. In general, their biodegradation takes place in two stages in which SF is first adsorbed onto enzymes and then digested by them. The final degradation products of SF are the corresponding amino acids which are readily absorbed [202]. Chymotrypsin degrades amorphous regions of fibroins to release highly crystallizable fibroin proteins [207]. Proteolytic enzymes can cleave the less crystalline regions of the protein to peptides which can be phagocytosed for further metabolism by the cell [208].

4.6. CD

CDs are annular oligosaccharides made up of various dextrose units [209]. They can improve water solubility, in vivo stability, and the delivery of drugs [210]. Extensive use of CDs in NC DDS is mainly due to their ability to: (a) avoid undesirable interactions between drugs and the physiological environment [211]; (b) promote drug adsorption by interacting with biomembranes [211]; (c) regulate drug release [212]; and (d) display minimal toxicity in clinical use [213].

Kubota et al. found that β-CD is absorbed from the GI tract in rat but to only a small extent due to its large MW and hydrophilic nature [214]. Nevertheless, the absorption is by passive diffusion [215]. Similarly, the oral bioavailability of hydroxypropyl-β-CD in human is very low at <1% [216]. After absorption, CDs distribute mainly to the kidney and to a lesser extent to bladder, liver and adrenal gland. Most CDs are eliminated from tissues soon after administration but methyl-β-CD is retained in the kidney for at least 6 days at an almost unchanged level. After absorption, most CDs remain in extracellular compartments and do not access deep compartments or storage pools. [215] The excretion of CDs is mainly via renal clearance that can lead to accumulation in the kidney with potential to cause renal impairment [217]. It has also been reported that derivatives of β-CD are cytotoxic to human Caco-2 cells and can cause lung inflammation and early fibrosis after infusion [19,20]. Clearly the safety of CD-based NCs needs further investigation.

Orally administered CDs are mainly metabolized by bacteria in the GI tract to produce oligosaccharides, monosaccharides and gases such as hydrogen, carbon dioxide and methane. After oral administration, γ-CD is almost completely digested in the GI tract. α-CD and β-CD are mainly digested by bacteria in the colon with α-CD being digested more slowly [217]. CDs administered by i.v. injection to rat are rapidly excreted unchanged via the kidney with some 90% of β-CD being recovered in urine. Absorbed CDs after oral administration are also excreted in the kidney but, in this case, only 0.6% of β-CD can be recovered in urine [214,215].

5. Conclusions and future perspectives

This review describes the ADME of the biomaterials (MDNS) that commonly make up NC DDS. In contrast to previous reviews dealing with the PK of the NCs themselves, its main focus is the PK of MDNS after their release from NCs and the various clearance mechanisms by which they are excreted. Safety is always the most important consideration for any medical product and is of particular concern in relation to MDNS since they are present in large amounts in NCs and, when released, have the potential to cause toxicity. For instance, poloxamers, PVPs and PEGs with high MW can accumulate in tissues and cause health problems. Hence, MDNS and their metabolites should be biodegradable and easily excreted. Moreover, some MDNS and their metabolites have bioactivity which may lead to undesirable effects. For example, acid metabolites of PEGs may cause acidosis and hypercalcemia; chitosan can reduce emulsification of lipids and promote platelet adhesion; and a metabolite of PLA can cause inflammatory tissue reactions. MDNS and their metabolites may also affect the function of drug transporters and metabolic enzymes leading to drug-MDNS interactions and potential toxicity. Therefore, inertness is a highly desirable feature of MDNS.

This review also describes the various bioanalytical methods used to evaluate the PK of NCs and MDNS. However, to date there are no standardized protocols for evaluating the ADME of NCs and MDNS resulting in problems when trying to compare the results of different studies [218]. Therefore, the development of evaluation standards has high priority.

Because of big differences in the PK of parenteral drugs and NC systems, a deep understanding of the ADME of MDNS is important to ensure the safe clinical use of NCs. Although much is known about the PK of drugs, more work is needed to reach the same level of insight into NC DDS. We hope this review will serve to promote this greater understanding.

Declaration of Competing Interest

The authors have no conflict of interest to declare.

Acknowledgements

The work is supported by the National Natural Science Foundation of China (Grant No. 81430087, 81673396, 81872831, and 81603182), and the Science and Technology Major Specialized Projects of China (Grant No. 2017ZX09101001, 2018ZX09721002-007).

(i.p. injection: intraperitoneal injection; HA: hyaluronic acid; NIR: near-infrared)

References

[1] M. Moros, S.G. Mitchell, V. Grazu, J.M. de la Fuente, The fate of nanocarriers as nanomedicines in vivo: important considerations and biological barriers to overcome, Curr. Med. Chem. 20 (2013) 2759–2778.
[2] M. Wacker, Nanocarriers for intravenous injection – the long hard road to the market, Int. J. Pharm. 457 (2013) 50–62.
[3] C. Ding, Z. Li, A review of drug release mechanisms from nanocarrier systems, Mater. Sci. Eng. C Mater. Biol. Appl. 76 (2017) 1440–1453.
[4] O.C. Farokhzad, R. Langer, Impact of nanotechnology on drug delivery, ACS Nano 3 (2009) 16–20.
[5] Z. Li, B.H. Tan, Towards the development of polycaprolactone based amphiphilic block copolymers: molecular design, self-assembly and biomedical applications, Mater. Sci. Eng. C Mater. Biol. Appl. 45 (2014) 620–634.
[6] M. Liu, H. Du, W. Zhang, G. Zhai, Internal stimuli-responsive nanocarriers for drug delivery: design strategies and applications, Mater. Sci. Eng. C Mater. Biol. Appl. 71 (2017) 1267–1280.
[7] A. Wicki, D. Witzigmann, V. Balasubramanian, J. Huwyler, Nanomedicine in cancer therapy: challenges, opportunities, and clinical applications, J. Control. Release 200 (2015) 138–157.
[8] C.B. Longley, H. Zhao, Y.L. Lozanguiez, C.D. Conover, Biodistribution and excretion of radiolabeled 40 kDa polyethylene glycol following intravenous administration in mice, J. Pharm. Sci. 102 (2013) 2362–2370.
[9] B.M. Johnson, W.N. Charman, C.J.H. Porter, An in vitro examination of the impact of polyethylene glycol 400, pluronic P85, and vitamin E d-α-tocopheryl polyethylene glycol 1000 succinate on P-glycoprotein efflux and enterocyte-based metabolism in excised rat intestine, AAPS PharmSci. 4 (2002) 193–205.
[10] E.D. Hugger, B.L. Novak, P.S. Burton, K.L. Audus, R.T. Borchardt, A comparison of commonly used polyethoxylated pharmaceutical excipients on their ability to inhibit P-glycoprotein activity in vitro, J. Pharm. Sci. 91 (2002) 1991–2002.
[11] Q. Shen, Y. Lin, T. Handa, M. Doi, M. Sugie, K. Wakayama, N. Okada, T. Fujita, A. Yamamoto, Modulation of intestinal P-glycoprotein function by polyethylene glycols and their derivatives by in vitro transport and in situ absorption studies, Int. J. Pharm. 313 (2006) 49.
[12] S. Devang, P. Sundeep, M. Muralikrishna, C. Gajendra, S. Murali, S. Ajay, G.S. Matthew, H. John, H. Roy, M. Punit, M. Sandhya, A systematic evaluation of solubility enhancing excipients to enable the generation of permeability data for poorly soluble compounds in Caco-2 model, Drug Metab. Lett. 8 (2014) 109–118.
[13] D.A. Ashiru-Oredope, N. Patel, B. Forbes, R. Patel, A.W. Basit, The effect of polyoxyethylene polymers on the transport of ranitidine in Caco-2 cell monolayers, Int. J. Pharm. 409 (2011) 164–168.

[14] R. Webster, E. Didier, P. Harris, N. Siegel, J. Stadler, L. Tilbury, D. Smith, PEGylated proteins: evaluation of their safety in the absence of definitive metabolism studies, Drug Metab. Dispos. 35 (2007) 9–16.
[15] R.Y. Li, Z.G. Liu, H.Q. Liu, L. Chen, J.F. Liu, Y.H. Pan, Evaluation of biocompatibility and toxicity of biodegradable poly (DL-lactic acid) films, Am. J. Transl. Res. 7 (2015) 1357–1370.
[16] H. Zhu, F. Yang, B. Tang, X.M. Li, Y.N. Chu, Y.L. Liu, S.G. Wang, D.C. Wu, Y. Zhang, Mesenchymal stem cells attenuated PLGA-induced inflammatory responses by inhibiting host DC maturation and function, Biomaterials 53 (2015) 688–698.
[17] M. Christensen, P. Johansen, C. Hau, Storage of polyvinylpyrrolidone (PVP) in tissues following long-term treatment with a PVP-containing vasopressin preparation, Acta Med. Scand. 204 (1978) 295–298.
[18] P. Li, J. Song, X. Ni, Q. Guo, H. Wen, Q. Zhou, Y. Shen, Y. Huang, P. Qiu, S. Lin, H. Hu, Comparison in toxicity and solubilizing capacity of hydroxypropyl-β-cyclodextrin with different degree of substitution, Int. J. Pharm. 513 (2016) 347–356.
[19] A.M. Tötterman, N.G. Schipper, D.O. Thompson, J.P. Mannermaa, Intestinal safety of water-soluble β-cyclodextrins in paediatric oral solutions of spironolactone: effects on human intestinal epithelial Caco-2 cells, J. Pharm. Pharmacol. 49 (1997) 43–48.
[20] M. Matsuo, H. Arima, T. Irie, Reply: lung toxicity of hydroxyl-β-cyclodextrin infusion, Mol. Genet. Metab. 109 (2013) 233.
[21] R. Ylitalo, S. Lehtinen, E. Wuolijoki, P. Ylitalo, T. Lehtimäki, Cholesterol-lowering properties and safety of chitosan, Arzneimittelforschung 52 (2002) 1–7.
[22] S.D. Ray, Potential aspects of chitosan as pharmaceutical excipient, Acta Pol. Pharm. 68 (2011) 619–622.
[23] M. Emanuele, B. Balasubramaniam, Differential effects of commercial-grade and purified poloxamer 188 on renal function, Drugs R. D. 14 (2014) 73–83.
[24] X.D. Zhang, D. Wu, X. Shen, P.X. Liu, F.Y. Fan, S.J. Fan, In vivo renal clearance, biodistribution, toxicity of gold nanoclusters, Biomaterials 33 (2012) 4628–4638.
[25] S.J.K. Jung Hwan Hwang, Yong-Hoon Kim, Jung-Ran Noh, Gil-Tae Gang, Bong Hyun Chung, Nam Woong Song, Chul-Ho Lee, Susceptibility to gold nanoparticle-induced hepatotoxicity is enhanced in a mouse model of nonalcoholic steatohepatitis, Toxicology 294 (2012) 27–35.
[26] S. Fraga, A. Brandão, M.E. Soares, T. Morais, J.A. Duarte, L. Pereira, L. Soares, C. Neves, E. Pereira, L. Bastos Mde, H. Carmo, Short- and long-term distribution and toxicity of gold nanoparticles in the rat after a single-dose intravenous administration, Nanomedicine 10 (2014) 1757–1766.
[27] D. Ali, H. Ali, S. Alarifi, S. Kumar, M. Serajuddin, A.P. Mashih, M. Ahmed, M. Khan, S.F. Adil, M.R. Shaik, A.A. Ansari, Impairment of DNA in a freshwater gastropod (*Lymnea luteola* L.) after exposure to titanium dioxide nanoparticles, Arch. Environ. Contam. Toxicol. 68 (2015) 543–552.
[28] J.K. Folkmann, L. Risom, N.R. Jacobsen, H. Wallin, S. Loft, P. Møller, Oxidatively damaged DNA in rats exposed by oral gavage to C60 fullerenes and single-walled carbon nanotubes, Environ. Health Perspect. 117 (2009) 703–708.
[29] L. Li, H. Wu, W.J. Peijnenburg, C.A. van Gestel, Both released silver ions and particulate Ag contribute to the toxicity of AgNPs to earthworm *Eisenia fetida*, Nanotoxicology 9 (2015) 792–801.
[30] A. Krawczyńska, K. Dziendzikowska, J. Gromadzka-Ostrowska, A. Lankoff, A.P. Herman, M. Oczkowski, T. Królikowski, J. Wilczak, M. Wojewódzka, M. Kruszewski, Silver and titanium dioxide nanoparticles alter oxidative/inflammatory response and renin-angiotensin system in brain, Food Chem. Toxicol. 85 (2015) 96–105.
[31] J. Shi, X. Sun, Y. Lin, X. Zou, Z. Li, Y. Liao, M. Du, H. Zhang, Endothelial cell injury and dysfunction induced by silver nanoparticles through oxidative stress via IKK/NF-κB pathways, Biomaterials 35 (2014) 6657–6666.
[32] K. Meyer, P. Rajanahalli, M. Ahamed, J.J. Rowe, Y. Hong, ZnO nanoparticles induce apoptosis in human dermal fibroblasts via p53 and p38 pathways, Toxicol, In Vitro 25 (2011) 1721–1726.
[33] X. Yang, Y. Li, Y. Li, X. Ren, X. Zhang, D. Hu, Y. Gao, Y. Xing, H. Shang, Oxidative stress-mediated atherosclerosis: mechanisms and therapies, Front. Physiol. 8 (2017) 600.
[34] J.G. Ayres, P. Borm, F.R. Cassee, V. Castranova, K. Donaldson, A. Ghio, R.M. Harrison, R. Hider, F. Kelly, I.M. Kooter, F. Marano, R.L. Maynard, I. Mudway, A. Nel, C. Sioutas, S. Smith, A. Baeza-Squiban, A. Cho, S. Duggan, J. Froines, Evaluating the toxicity of airborne particulate matter and nanoparticles by measuring oxidative stress potential – a workshop report and consensus statement, Inhal. Toxicol. 20 (2008) 75.
[35] D. Han, Y. Tian, Z. Tao, G. Ren, Y. Zhuo, Nano-zinc oxide damages spatial cognition capability via over-enhanced long-term potentiation in hippocampus of Wistar rats, Int. J. Nanomedicine 6 (2011) 1453–1461.
[36] S.T. Yang, X. Wang, G. Jia, Y. Gu, T. Wang, H. Nie, C. Ge, H. Wang, Y. Liu, Long-term accumulation and low toxicity of single-walled carbon nanotubes in intravenously exposed mice, Toxicol. Lett. 181 (2008) 182–189.
[37] L. Giodini, F.L. Re, D. Campagnol, E. Marangon, B. Posocco, E. Dreussi, G. Toffoli, Nanocarriers in cancer clinical practice: a pharmacokinetic issue, Nanomedicine 13 (2017) 583–599.
[38] V.A. Galievsky, A.S. Stasheuski, S.N. Krylov, Improvement of LOD in fluorescence detection with spectrally nonuniform background by optimization of emission filtering, Anal. Chem. 89 (2017) 11122–11128.
[39] C. Su, Y. Liu, Y. He, J. Gu, Analytical methods for investigating in vivo fate of nanoliposomes: a review, J. Pharm. Anal. 8 (2018) 219–225.
[40] A. Schädlich, T. Naolou, E. Amado, R. Schöps, J. Kressler, K. Mäder, Noninvasive in vivo monitoring of the biofate of 195 kDa poly(vinyl alcohol) by multispectral fluorescence imaging, Biomacromolecules 12 (2011) 3674–3683.
[41] Y. Jiang, A. Schädlich, E. Amado, C. Weis, E. Odermatt, K. Mäder, J. Kressler, In-vivo studies on intraperitoneally administrated poly(vinyl alcohol), J Biomed Mater Res B Appl Biomater 93 (2010) 275–284.
[42] W. Dong, B. Han, K. Shao, Z. Yang, Y. Peng, Y. Yang, W. Liu, Effects of molecular weights on the absorption, distribution and urinary excretion of intraperitoneally administrated carboxymethyl chitosan in rats, J. Mater. Sci. Mater. Med. 23 (2012) 2945–2952.
[43] C. Kuehl, T. Zhang, L.M. Kaminskas, C.J. Porter, N.M. Davies, L. Forrest, C. Berkland, Hyaluronic acid molecular weight determines lung clearance and biodistribution after instillation, Mol. Pharm. 13 (2016) 1904–1914.
[44] E.J. Oh, K. Park, K.S. Kim, J. Kim, J.A. Yang, J.H. Kong, M.Y. Lee, A.S. Hoffman, S.K. Hahn, Target specific and long-acting delivery of protein, peptide, and nucleotide therapeutics using hyaluronic acid derivatives, J. Control. Release 141 (2010) 2–12.
[45] S. Kadi, D. Cui, E. Bayma, T. Boudou, C. Nicolas, K. Glinel, C. Picart, R. Auzély-Velty, Alkylamino hydrazide derivatives of hyaluronic acid: synthesis, characterization in semidilute aqueous solutions, and assembly into thin multilayer films, Biomacromolecules 10 (2009) 2875–2884.
[46] G.D. Prestwich, D.M. Marecak, J.F. Marecek, K.P. Vercruysse, M.R. Ziebell, Controlled chemical modification of hyaluronic acid: synthesis, applications, and biodegradation of hydrazide derivatives, J. Control. Release 53 (1998) 93–103.
[47] G. Bastiat, C.O. Pritz, C. Roider, F. Fouchet, E. Lignières, A. Jesacher, R. Glueckert, M. Ritsch-Marte, A. Schrott-Fischer, P. Saulnier, J.P. Benoit, A new tool to ensure the fluorescent dye labeling stability of nanocarriers: a real challenge for fluorescence imaging, J. Control. Release 170 (2013) 334–342.
[48] C. Chen, Y.F. Li, Y. Qu, Z. Chai, Y. Zhao, Advanced nuclear analytical and related techniques for the growing challenges in nanotoxicology, Chem. Soc. Rev. 42 (2013) 8266–8303.
[49] J.M. Grindel, T. Jaworski, O. Piraner, R.M. Emanuele, M. Balasubramanian, Distribution, metabolism, and excretion of a novel surface-active agent, purified poloxamer 188, in rats, dogs, and humans, J. Pharm. Sci. 91 (2002) 1936–1947.
[50] M. Laznicek, A. Laznickova, D. Cozikova, V. Velebny, Preclinical pharmacokinetics of radiolabelled hyaluronan, Pharmacol. Rep. 64 (2012) 428–437.
[51] L. Balogh, A. Polyak, D. Mathe, R. Kiraly, J. Thuroczy, M. Terez, G. Janoki, Y. Ting, L.R. Bucci, A.G. Schauss, Absorption, uptake and tissue affinity of high-molecular-weight hyaluronan after oral administration in rats and dogs, J. Agric. Food Chem. 56 (2008) 10582–10593.
[52] D. Cozikova, A. Laznickova, M. Hermannova, E. Svanovsky, L. Palek, R. Buffa, P. Sedova, R. Koppova, M. Petrik, D. Smejkalova, M. Laznicek, V. Velebny, Preparation and the kinetic stability of hyaluronan radiolabeled with ^{111}In, ^{125}I and ^{14}C, J. Pharm. Biomed. Anal. 52 (2010) 517–524.
[53] C. Alric, I. Miladi, D. Kryza, J. Taleb, F. Lux, R. Bazzi, C. Billotey, M. Janier, P. Perriat, S. Roux, O. Tillement, The biodistribution of gold nanoparticles designed for renal clearance, Nanoscale 5 (2013) 5930–5939.
[54] H. Hwang, K.I. Kim, J. Kwon, B.S. Kim, H.S. Jeong, S.J. Jang, S. Oh, H.S. Park, S.T. Lim, M.H. Sohn, H.J. Jeong, (131)I-labeled chitosan hydrogels for radioembolization: a preclinical study in small animals, Nucl. Med. Biol. 52 (2017) 16–23.
[55] M. Becker, N. Balagué, X. Montet, A. Calmy, D. Salomon, L. Toutous-Trellu, Hyaluronic acid filler in HIV-associated facial lipoatrophy: evaluation of tissue distribution and morphology with MRI, Dermatology 230 (2015) 367–374.
[56] R.J. Rohrich, J.E. Pessa, The fat compartments of the face: anatomy and clinical implications for cosmetic surgery, Plast. Reconstr. Surg. 119 (2007) 2219–2227.
[57] Z. Chen, C. Yan, S. Yan, Q. Liu, M. Hou, Y. Xu, R. Guo, Non-invasive monitoring of in vivo hydrogel degradation and cartilage regeneration by multiparametric MR imaging, Theranostics 8 (2018) 1146–1158.
[58] C.T. Quinn, T.G. St Pierre, MRI measurements of iron load in transfusion-dependent patients: implementation, challenges, and pitfalls, Pediatr. Blood Cancer 63 (2016) 773–780.
[59] J.M. Grindel, T. Jaworski, R.M. Emanuele, P. Culbreth, Pharmacokinetics of a novel surface-active agent, purified poloxamer 188, in rat, rabbit, dog and man, Biopharm. Drug Dispos. 23 (2002) 87–103.
[60] A.K. Mohammad, J.J. Reineke, Quantitative detection of PLGA nanoparticle degradation in tissues following intravenous administration, Mol. Pharm. 10 (2013) 2183–2189.
[61] Z. Gajdosechova, Z. Mester, Recent trends in analysis of nanoparticles in biological matrices, Anal. Bioanal. Chem. (2019) https://doi.org/10.1007/s00216-019-01620-9.
[62] Y. Lee, J. Choi, P. Kim, K. Choi, S. Kim, W. Shon, K. Park, A transfer of silver nanoparticles from pregnant rat to offspring, Toxicol. Res. 28 (2012) 139–141.
[63] M. Salimi, S. Sarkar, S. Fathi, A.M. Alizadeh, R. Saber, F. Moradi, H. Delavari, Biodistribution, pharmacokinetics, and toxicity of dendrimer-coated iron oxide nanoparticles in BALB/c mice, Int. J. Nanomedicine 13 (2018) 1483–1493.
[64] J. Gong, X. Gu, W.E. Achanzar, K.D. Chadwick, J. Gan, B.J. Brock, N.S. Kishnani, W.G. Humphreys, R.A. Iyer, Quantitative analysis of polyethylene glycol (PEG) and PEGylated proteins in animal tissues by LC-MS/MS coupled with in-source CID, Anal. Chem. 86 (2014) 7642–7649.
[65] X. Zhou, X. Meng, L. Cheng, C. Su, Y. Sun, L. Sun, Z. Tang, J.P. Fawcett, Y. Yang, J. Gu, Development and application of an MS(ALL)-based approach for the quantitative analysis of linear polyethylene glycols in rat plasma by liquid chromatography triple-quadrupole/time-of-flight mass spectrometry, Anal. Chem. 89 (2017) 5193–5200.
[66] L. Yin, C. Su, T. Ren, X. Meng, M. Shi, J. Paul Fawcett, M. Zhang, W. Hu, J. Gu, MS(All) strategy for comprehensive quantitative analysis of PEGylated-doxorubicin, PEG and doxorubicin by LC-high resolution q-q-TOF mass spectrometry coupled with all window acquisition of all fragment ion spectra, Analyst 142 (2017) 4279–4288.
[67] H. Sun, Q. Zhang, Z. Zhang, J. Tong, D. Chu, J. Gu, Simultaneous quantitative analysis of polyethylene glycol (PEG), PEGylated paclitaxel and paclitaxel in rats by MS/MS (ALL) technique with hybrid quadrupole time-of-flight mass spectrometry, J. Pharm. Biomed. Anal. 145 (2017) 255–261.

[68] M. Hamidi, A. Azadi, P. Rafiei, H. Ashrafi, A pharmacokinetic overview of nanotechnology-based drug delivery systems: an ADME-oriented approach, Crit. Rev. Ther. Drug Carrier Syst. 30 (2013) 435–467.
[69] S.D. Li, L. Huang, Pharmacokinetics and biodistribution of nanoparticles, Mol. Pharm. 5 (2008) 496–504.
[70] L. Wang, L. Yan, J. Liu, C. Chen, Y. Zhao, Quantification of nanomaterial/nanomedicine trafficking in vivo, Anal. Chem. 90 (2018) 589–614.
[71] M. Li, K.T. Al-Jamal, K. Kostarelos, J. Reineke, Physiologically based pharmacokinetic modeling of nanoparticles, ACS Nano 4 (2010) 6303–6317.
[72] O. Veiseh, J.W. Gunn, M. Zhang, Design and fabrication of magnetic nanoparticles for targeted drug delivery and imaging, Adv. Drug Deliv. Rev. 62 (2010) 284–304.
[73] B.T. Griffin, J. Guo, E. Presas, M.D. Donovan, M.J. Alonso, C.M. O'Driscoll, Pharmacokinetic, pharmacodynamic and biodistribution following oral administration of nanocarriers containing peptide and protein drugs, Adv. Drug Deliv. Rev. 106 (2016) 367–380.
[74] T.W. Prow, J.E. Grice, L.L. Lin, R. Faye, M. Butler, W. Becker, E.M. Wurm, C. Yoong, T.A. Robertson, H.P. Soyer, M.S. Roberts, Nanoparticles and microparticles for skin drug delivery, Adv. Drug Deliv. Rev. 63 (2011) 470–491.
[75] A.E. Nel, L. Mädler, D. Velegol, T. Xia, E.M. Hoek, P. Somasundaran, F. Klaessig, V. Castranova, M. Thompson, Understanding biophysicochemical interactions at the nano-bio interface, Nat. Mater. 8 (2009) 543–557.
[76] N. Bertrand, J.C. Leroux, The journey of a drug-carrier in the body: an anatomo-physiological perspective, J. Control. Release 161 (2012) 152–163.
[77] W.H. De Jong, W.I. Hagens, P. Krystek, M.C. Burger, A.J. Sips, R.E. Geertsma, Particle size-dependent organ distribution of gold nanoparticles after intravenous administration, Biomaterials 29 (2008) 1912–1919.
[78] S.M. Moghimi, A.C. Hunter, J.C. Murray, Long-circulating and target-specific nanoparticles: theory to practice, Pharmacol. Rev. 53 (2001) 283–318.
[79] X. Zhang, X. Yang, J. Ji, A. Liu, G. Zhai, Tumor targeting strategies for chitosan-based nanoparticles, Colloids Surf. B: Biointerfaces 148 (2016) 460–473.
[80] N. Daum, C. Tscheka, A. Neumeyer, M. Schneider, Novel approaches for drug delivery systems in nanomedicine: effects of particle design and shape, Wiley Interdiscip. Rev. Nanomed. Nanobiotechnol. 4 (2012) 52–65.
[81] W. Wang, C.Y. Tong, X.Y. Liu, T. Li, B. Liu, W. Xiong, Preparation and functional characterization of tumor-targeted folic acid-chitosan conjugated nanoparticles loaded with mitoxantrone, J. Cent. South Univ. 22 (2015) 3311–3317.
[82] A. Dasargyri, P. Hervella, A. Christiansen, S.T. Proulx, M. Detmar, J.C. Leroux, Findings questioning the involvement of Sigma-1 receptor in the uptake of anisamide-decorated particles, J. Control. Release 224 (2016) 229–238.
[83] N.K. Garg, P. Dwivedi, C. Campbell, R.K. Tyagi, Site specific/targeted delivery of gemcitabine through anisamide anchored chitosan/poly ethylene glycol nanoparticles: an improved understanding of lung cancer therapeutic intervention, Eur. J. Pharm. Sci. 47 (2012) 1006–1014.
[84] K.A. Fitzgerald, M. Malhotra, M. Gooding, F. Sallas, J.C. Evans, R. Darcy, C.M. O'Driscoll, A novel, anisamide-targeted cyclodextrin nanoformulation for siRNA delivery to prostate cancer cells expressing the sigma-1 receptor, Int. J. Pharm. 499 (2016) 131–145.
[85] J. Guo, J.R. Ogier, S. Desgranges, R. Darcy, C. O'Driscoll, Anisamide-targeted cyclodextrin nanoparticles for siRNA delivery to prostate tumours in mice, Biomaterials 33 (2012) 7775–7784.
[86] L. Zhang, J.P. Zhou, J. Yao, Improved anti-tumor activity and safety profile of a paclitaxel-loaded glycyrrhetinic acid-graft-hyaluronic acid conjugate as a synergistically targeted drug delivery system, Chin. J. Nat. Med. 13 (2015) 915–924.
[87] A.A. D'Souza, P.V. Devarajan, Asialoglycoprotein receptor mediated hepatocyte targeting - strategies and applications, J. Control. Release 203 (2015) 126–139.
[88] M. Michael, M.M. Doherty, Tumoral drug metabolism: overview and its implications for cancer therapy, J. Clin. Oncol. 23 (2005) 205–229.
[89] B. Ballou, L.A. Ernst, S. Andreko, T. Harper, J.A. Fitzpatrick, A.S. Waggoner, M.P. Bruchez, Sentinel lymph node imaging using quantum dots in mouse tumor models, Bioconjug. Chem. 18 (2007) 389–396.
[90] I. Iavicoli, V. Leso, L. Fontana, A. Bergamaschi, Toxicological effects of titanium dioxide nanoparticles: a review of in vitro mammalian studies, Eur. Rev. Med. Pharmacol. Sci. 15 (2011) 481–508.
[91] K. Klien, J. Godnić-Cvar, Genotoxicity of metal nanoparticles: focus on in vivo studies, Arh. Hig. Rada. Toksikol. 63 (2012) 133–145.
[92] L. Li, L. Hu, Q. Zhou, C. Huang, Y. Wang, C. Sun, G. Jiang, Sulfidation as a natural antidote to metallic nanoparticles is overestimated: CuO sulfidation yields CuS nanoparticles with increased toxicity in medaka (*Oryzias latipes*) embryos, Environ. Sci. Technol. 49 (2015) 2486–2495.
[93] Q. Sun, M. Radosz, Y. Shen, Challenges in design of translational nanocarriers, J. Control. Release 164 (2012) 156–169.
[94] K. Zarschler, L. Rocks, N. Licciardello, L. Boselli, E. Polo, K.P. Garcia, L. De Cola, H. Stephan, K.A. Dawson, Ultrasmall inorganic nanoparticles: state-of-the-art and perspectives for biomedical applications, Nanomedicine 12 (2016) 1663–1701.
[95] A.A. Vlasova II, Z.P. Kapralov, S.C. Michael, M.R. Burkert, A. Shurin, A.A. Star, V.E. Kagan Shvedova, Enzymatic oxidative biodegradation of nanoparticles: mechanisms, significance and applications, Toxicol. Appl. Pharmacol. 299 (2016) 58–69.
[96] A.R. Sureshbabu, R. Kurapati, J. Russier, C. Ménard-Moyon, I. Bartolini, M. Meneghetti, K. Kostarelos, A. Bianco, Degradation-by-design: surface modification with functional substrates that enhance the enzymatic degradation of carbon nanotubes, Biomaterials 72 (2015) 20–28.
[97] M. Yu, J. Zheng, Clearance pathways and tumor targeting of imaging nanoparticles, ACS Nano 9 (2015) 6655–6674.
[98] X. Liang, H. Wang, Y. Zhu, R. Zhang, V.C. Cogger, X. Liu, Z.P. Xu, J.E. Grice, M.S. Roberts, Short- and long-term tracking of anionic ultrasmall nanoparticles in kidney, ACS Nano 10 (2016) 387–395.
[99] L.Y. Chou, H.C. Fischer, S.D. Perrault, W.C. Chan, Visualizing quantum dots in biological samples using silver staining, Anal. Chem. 81 (2009) 4560–4565.
[100] S.S. Nigavekar, L.Y. Sung, M. Llanes, A. El-Jawahri, T.S. Lawrence, C.W. Becker, L. Balogh, M.K. Khan, 3H dendrimer nanoparticle organ/tumor distribution, Pharm. Res. 21 (2004) 476–483.
[101] I. Ellinger, R. Fuchs, Receptor-mediated and fluid-phase transcytosis of horseradish peroxidase across rat hepatocytes, J. Biomed. Biotechnol. (2010) (2010), 850320.
[102] S. Friman, B. Egestad, J. Sjövall, J. Svanvik, Hepatic excretion and metabolism of polyethylene glycols and mannitol in the cat, J. Hepatol. 17 (1993) 48–55.
[103] K. Furumoto, K. Ogawara, M. Yoshida, Y. Takakura, M. Hashida, K. Higaki, T. Kimura, Biliary excretion of polystyrene microspheres depends on the type of receptor-mediated uptake in rat liver, Biochim. Biophys. Acta 1526 (2001) 221–226.
[104] W.G. Hardison, P.J. Lowe, M. Shanahan, Effect of molecular charge on Para- and transcellular access of horseradish peroxidase into rat bile, Hepatology 9 (1989) 866–871.
[105] M. Hashida, R. Atsumi, K. Nishida, S. Nakane, Y. Takakura, H. Sezaki, Biliary excretion of mitomycin C dextran conjugates in relation to physicochemical characteristics of carrier dextran, Aust. J. Pharm. 13 (1990) 441–447.
[106] B.D. Ulery, L.S. Nair, C.T. Laurencin, Biomedical applications of biodegradable polymers, J. Polym. Sci. B Polym. Phys. 49 (2011) 832–864.
[107] J.C. Middleton, A.J. Tipton, Synthetic biodegradable polymers as orthopedic devices, Biomaterials 21 (2000) 2335–2346.
[108] A.C. Albertsson, I.K. Varma, Recent developments in ring opening polymerization of lactones for biomedical applications, Biomacromolecules 4 (2003) 1466–1486.
[109] S.K. Pandey, D.K. Patel, R. Thakur, D.P. Mishra, P. Maiti, C. Haldar, Anti-cancer evaluation of quercetin embedded PLA nanoparticles synthesized by emulsified nanoprecipitation, Int. J. Biol. Macromol. 75 (2015) 521–529.
[110] F. Sadat Tabatabaei Mirakabad, K. Nejati-Koshki, A. Akbarzadeh, M.R. Yamchi, M. Milani, N. Zarghami, V. Zeighamian, A. Rahimzadeh, S. Alimohammadi, Y. Hanifehpour, S.W. Joo, PLGA-based nanoparticles as cancer drug delivery systems, Asian Pac. J. Cancer Prev. 15 (2014) 517–535.
[111] S. Acharya, S.K. Sahoo, PLGA nanoparticles containing various anticancer agents and tumour delivery by EPR effect, Adv. Drug Deliv. Rev. 63 (2011) 170–183.
[112] M. Korang-Yeboah, Y. Gorantla, S.A. Paulos, P. Sharma, J. Chaudhary, R. Palaniappan, Polycaprolactone/maltodextrin nanocarrier for intracellular drug delivery: formulation, uptake mechanism, internalization kinetics, and subcellular localization, Int. J. Nanomedicine 10 (2015) 4763–4781.
[113] T.K. Dash, V.B. Konkimalla, Poly-small je, Ukrainian-caprolactone based formulations for drug delivery and tissue engineering: a review, J. Control. Release 158 (2012) 15–33.
[114] H. Sun, L. Mei, C. Song, X. Cui, P. Wang, The in vivo degradation, absorption and excretion of PCL-based implant, Biomaterials 27 (2006) 1735–1740.
[115] S.M. Navarro, T.W. Morgan, C.E. Astete, R.W. Stout, D. Coulon, P. Mottram, C.M. Sabliov, Biodistribution and toxicity of orally administered poly (lactic-co-glycolic) acid nanoparticles to F344 rats for 21 days, Nanomedicine (London) 11 (2016) 1653–1669.
[116] W. Zhang, J. Gao, Q. Zhu, M. Zhang, X. Ding, X. Wang, X. Hou, W. Fan, B. Ding, X. Wu, X. Wang, S. Gao, Penetration and distribution of PLGA nanoparticles in the human skin treated with microneedles, Int. J. Pharm. 402 (2010) 205–212.
[117] B. Semete, L. Booysen, Y. Lemmer, L. Kalombo, L. Katata, J. Verschoor, H.S. Swai, In vivo evaluation of the biodistribution and safety of PLGA nanoparticles as drug delivery systems, Nanomedicine 6 (2010) 662–671.
[118] J.K. Park, T. Utsumi, Y.E. Seo, Y. Deng, A. Satoh, W.M. Saltzman, Y. Iwakiri, Cellular distribution of injected PLGA-nanoparticles in the liver, Nanomedicine 12 (2016) 1365–1374.
[119] G. Schwach, M. Vert, In vitro and in vivo degradation of lactic acid-based interference screws used in cruciate ligament reconstruction, Int. J. Biol. Macromol. 25 (1999) 283–291.
[120] S.H. Lee, W.S. Song, Enzymatic hydrolysis of polylactic acid fiber, Appl. Biochem. Biotechnol. 164 (2011) 89–102.
[121] T. Beslikas, I. Gigis, V. Goulios, J. Christoforides, G.Z. Papageorgiou, D.N. Bikiaris, Crystallization study and comparative in vitro-in vivo hydrolysis of PLA reinforcement ligament, Int. J. Mol. Sci. 12 (2011) 6597–6618.
[122] W. Heidemann, S. Jeschkeit, K. Ruffieux, J.H. Fischer, M. Wagner, G. Kruger, E. Wintermantel, K.L. Gerlach, Degradation of poly(D,L)lactide implants with or without addition of calciumphosphates in vivo, Biomaterials 22 (2001) 2371–2381.
[123] J. Klompmaker, H.W. Jansen, R.P. Veth, J.H. de Groot, A.J. Nijenhuis, A.J. Pennings, Porous polymer implant for repair of meniscal lesions: a preliminary study in dogs, Biomaterials 12 (1991) 810–816.
[124] M.S. Taylor, A.U. Daniels, K.P. Andriano, J. Heller, Six bioabsorbable polymers: in vitro acute toxicity of accumulated degradation products, J. Appl. Biomater. 5 (1994) 151–157.
[125] R. Dinarvand, N. Sepehri, S. Manoochehri, H. Rouhani, F. Atyabi, Polylactide-co-glycolide nanoparticles for controlled delivery of anticancer agents, Int. J. Nanomedicine 6 (2011) 877–895.
[126] J. Singh, S. Desai, S. Yadav, B. Narasimhan, H. Kaur, Polymer drug conjugates: recent advancements in various diseases, Curr. Pharm. Des. 22 (2016) 2821–2843.
[127] A. Kolate, D. Baradia, S. Patil, I. Vhora, G. Kore, A. Misra, PEG - a versatile conjugating ligand for drugs and drug delivery systems, J. Control. Release 192 (2014) 67–81.
[128] G. Dumortier, J.L. Grossiord, F. Agnely, J.C. Chaumeil, A review of poloxamer 407 pharmaceutical and pharmacological characteristics, Pharm. Res. 23 (2006) 2709–2728.

[129] F. Yan, C. Zhang, Y. Zheng, L. Mei, L. Tang, C. Song, H. Sun, L. Huang, The effect of poloxamer 188 on nanoparticle morphology, size, cancer cell uptake, and cytotoxicity, Nanomedicine 6 (2010) 170–178.
[130] D. Jain, R. Athawale, A. Bajaj, S. Shrikhande, P.N. Goel, R.P. Gude, Studies on stabilization mechanism and stealth effect of poloxamer 188 onto PLGA nanoparticles, Colloids Surf. B: Biointerfaces 109 (2013) 59–67.
[131] K. Knop, R. Hoogenboom, D. Fischer, U.S. Schubert, Poly(ethylene glycol) in drug delivery: pros and cons as well as potential alternatives, Angew. Chem. Int. Ed. Eng. 49 (2010) 6288–6308.
[132] A. Baumann, D. Tuerck, S. Prabhu, L. Dickmann, J. Sims, Pharmacokinetics, metabolism and distribution of PEGs and PEGylated proteins: quo vadis? Drug Discov. Today 19 (2014) 1623–1631.
[133] R.W. Pelham, L.C. Nix, R.E. Chavira, M.V. Cleveland, P. Stetson, Clinical trial: single- and multiple-dose pharmacokinetics of polyethylene glycol (PEG-3350) in healthy young and elderly subjects, Aliment. Pharmacol. Ther. 28 (2008) 256–265.
[134] C. Fruijtier-Pölloth, Safety assessment on polyethylene glycols (PEGs) and their derivatives as used in cosmetic products, Toxicology 214 (2005) 1–38.
[135] D.G. Rudmann, J.T. Alston, J.C. Hanson, S. Heidel, High molecular weight polyethylene glycol cellular distribution and PEG-associated cytoplasmic vacuolation is molecular weight dependent and does not require conjugation to proteins, Toxicol. Pathol. 41 (2013) 970–983.
[136] T. Yamaoka, Y. Tabata, Y. Ikada, Distribution and tissue uptake of poly(ethylene glycol) with different molecular weights after intravenous administration to mice, J. Pharm. Sci. 83 (1994) 601–606.
[137] F.M. Veronese, G. Pasut, PEGylation, successful approach to drug delivery, Drug Discov. Today 10 (2005) 1451–1458.
[138] L. Yin, Cellular and systemic pharmacokinetics study of pegylated doxorubicin, Jilin University PhD thesis, 2018 , (In Chinese).
[139] H.P. Sun, Research on the nano-pharmacokinetics of PEGlyated Paclitaxel, Jilin University PhD thesis, 2017 , (In Chinese).
[140] S. Friman, J. Svanvik, Biliary excretion of 400- to 1,000-d polyethylene glycol will influence the calculation of small intestinal absorption in portacaval-shunted rats, Hepatology 25 (1997) 500.
[141] C.B. Shaffer, F.H. Critchfield, The absorption and excretion of the solid polyethylene glycols; (carbowax compounds), J. Am. Pharm. Assoc. Am. Pharm. Assoc. 36 (1947) 152–157.
[142] C.B. Shaffer, F.H. Critchfield, J.H. Nair 3rd, The absorption and excretion of a liquid polyethylene glycol, J. Am. Pharm. Assoc. Am. Pharm. Assoc. 39 (1950) 340–344.
[143] S. Friman, G. Radberg, J. Svanvik, Hepatic clearance of polyethylene glycol 900 and mannitol in the pig, Digestion 39 (1988) 172–180.
[144] M.G. Roma, R.A. Marinelli, E.A. Rodriguez Garay, Biliary excretion of polyethylene glycol molecular weight 900. Evidence for a bile salt-stimulated vesicular transport mechanism, Biochem. Pharmacol. 42 (1991) 1775–1781.
[145] X. Wei, Z. Zhang, Z. Qian, Pharmacokinetics and in vivo fate of drug loaded chitosan nanoparticles, Curr. Drug Metab. 13 (2012) 364–371.
[146] M.R. Kasaai, Various methods for determination of the degree of N-acetylation of chitin and chitosan: a review, J. Agric. Food Chem. 57 (2009) 1667–1676.
[147] M. Thanou, J.C. Verhoef, H.E. Junginger, Oral drug absorption enhancement by chitosan and its derivatives, Adv. Drug Deliv. Rev. 52 (2001) 117–126.
[148] W. Dong, B. Han, Y. Feng, F. Song, J. Chang, H. Jiang, Y. Tang, W. Liu, Pharmacokinetics and biodegradation mechanisms of a versatile carboxymethyl derivative of chitosan in rats: in vivo and in vitro evaluation, Biomacromolecules 11 (2010) 1527–1533.
[149] L. Illum, Chitosan and its use as a pharmaceutical excipient, Pharm. Res. 15 (1998) 1326–1331.
[150] I. Wedmore, J.G. McManus, A.E. Pusateri, J.B. Holcomb, A special report on the chitosan-based hemostatic dressing: experience in current combat operations, J. Trauma 60 (2006) 655–658.
[151] J. Vinsova, E. Vavrikova, Recent advances in drugs and prodrugs design of chitosan, Curr. Pharm. Des. 14 (2008) 1311–1326.
[152] J.H. Park, G. Saravanakumar, K. Kim, I.C. Kwon, Targeted delivery of low molecular drugs using chitosan and its derivatives, Adv. Drug Deliv. Rev. 62 (2010) 28–41.
[153] J.S. Park, T.H. Han, K.Y. Lee, S.S. Han, J.J. Hwang, D.H. Moon, S.Y. Kim, Y.W. Cho, N-acetyl histidine-conjugated glycol chitosan self-assembled nanoparticles for intracytoplasmic delivery of drugs: endocytosis, exocytosis and drug release, J. Control. Release 115 (2006) 37–45.
[154] L. Zhu, J. Ma, N. Jia, Y. Zhao, H. Shen, Chitosan-coated magnetic nanoparticles as carriers of 5-fluorouracil: preparation, characterization and cytotoxicity studies, Colloids Surf. B: Biointerfaces 68 (2009) 1–6.
[155] L. Robert, Hyaluronan, a truly "youthful" polysaccharide. Its medical applications, Pathol. Biol. (Paris) 63 (2015) 32–34.
[156] S. Arpicco, G. De Rosa, E. Fattal, Lipid-based nanovectors for targeting of CD44-overexpressing tumor cells, J. Drug Deliv. 2013 (2013), 860780.
[157] S. Ganesh, A.K. Iyer, D.V. Morrissey, M.M. Amiji, Hyaluronic acid based self-assembling nanosystems for CD44 target mediated siRNA delivery to solid tumors, Biomaterials 34 (2013) 3489–3502.
[158] S. Ganesh, A.K. Iyer, J. Weiler, D.V. Morrissey, M.M. Amiji, Combination of siRNA-directed gene silencing with cisplatin reverses drug resistance in human non-small cell lung cancer, Mol. Ther. Nucleic Acids 2 (2013) e110.
[159] L. Meléndez-Alafort, A. Nadali, E. Zangoni, A. Banzato, M. Rondina, A. Rosato, U. Mazzi, Biokinetic and dosimetric studies of 188Re-hyaluronic acid: a new radiopharmaceutical for treatment of hepatocellular carcinoma, Nucl. Med. Biol. 36 (2009) 693–701.
[160] H. Onishi, Y. Machida, Biodegradation and distribution of water-soluble chitosan in mice, Biomaterials 20 (1999) 175–182.
[161] Y. Kato, H. Onishi, Y. Machida, Biological fate of highly-succinylated N-succinyl-chitosan and antitumor characteristics of its water-soluble conjugate with mitomycin C at i.v. and i.p. administration into tumor-bearing mice, Biol. Pharm. Bull. 23 (2000) 1497–1503.
[162] S.Y. Chae, M.K. Jang, J.W. Nah, Influence of molecular weight on oral absorption of water soluble chitosans, J. Control. Release 102 (2005) 383–394.
[163] T. Kean, M. Thanou, Biodegradation, biodistribution and toxicity of chitosan, Adv. Drug Deliv. Rev. 62 (2010) 3–11.
[164] M. Oe, K. Mitsugi, W. Odanaka, H. Yoshida, Dietary hyaluronic acid migrates into the skin of rats, ScientificWorldJournal 2014 (2014), 378024.
[165] M. Kimura, T. Maeshima, T. Kubota, H. Kurihara, Y. Masuda, Y. Nomura, Absorption of orally administered hyaluronan, J. Med. Food 19 (2016) 1172–1179.
[166] S.C. Richardson, H.V. Kolbe, R. Duncan, Potential of low molecular mass chitosan as a DNA delivery system: biocompatibility, body distribution and ability to complex and protect DNA, Int. J. Pharm. 178 (1999) 231–243.
[167] C. Zhang, G. Qu, Y. Sun, X. Wu, Z. Yao, Q. Guo, Q. Ding, S. Yuan, Z. Shen, Q. Ping, H. Zhou, Pharmacokinetics, biodistribution, efficacy and safety of N-octyl-O-sulfate chitosan micelles loaded with paclitaxel, Biomaterials 29 (2008) 1233–1241.
[168] F. Alexis, E. Pridgen, L.K. Molnar, O.C. Farokhzad, Factors affecting the clearance and biodistribution of polymeric nanoparticles, Mol. Pharm. 5 (2008) 505–515.
[169] A.K. Gupta, M. Gupta, Synthesis and surface engineering of iron oxide nanoparticles for biomedical applications, Biomaterials 26 (2005) 3995–4021.
[170] T. Banerjee, A.K. Singh, R.K. Sharma, A.N. Maitra, Labeling efficiency and biodistribution of technetium-99m labeled nanoparticles: interference by colloidal tin oxide particles, Int. J. Pharm. 289 (2005) 189–195.
[171] C. Zhang, G. Qu, Y. Sun, T. Yang, Z. Yao, W. Shen, Z. Shen, Q. Ding, H. Zhou, Q. Ping, Biological evaluation of N-octyl-O-sulfate chitosan as a new nano-carrier of intravenous drugs, Eur. J. Pharm. Sci. 33 (2008) 415–423.
[172] M.N. Courel, C. Maingonnat, P. Bertrand, C. Chauzy, F. Smadja-Joffe, B. Delpech, Biodistribution of injected tritiated hyaluronic acid in mice: a comparison between macromolecules and hyaluronic acid-derived oligosaccharides, In Vivo 18 (2004) 181–187.
[173] J.D. Funkhouser, N.N. Aronson Jr., Chitinase family GH18: evolutionary insights from the genomic history of a diverse protein family, BMC Evol. Biol. 7 (2007) 96.
[174] Z. Guo, R. Chen, R. Xing, S. Liu, H. Yu, P. Wang, C. Li, P. Li, Novel derivatives of chitosan and their antifungal activities in vitro, Carbohydr. Res. 341 (2006) 351–354.
[175] D. Jiang, J. Liang, P.W. Noble, Hyaluronan in tissue injury and repair, Annu. Rev. Cell Dev. Biol. 23 (2007) 435–461.
[176] S.P. Evanko, T.N. Wight, Intracellular localization of hyaluronan in proliferating cells, J. Histochem. Cytochem. 47 (1999) 1331–1342.
[177] K. Yamazaki, K. Fukuda, M. Matsukawa, F. Hara, K. Yoshida, M. Akagi, H. Munakata, C. Hamanishi, Reactive oxygen species depolymerize hyaluronan: involvement of the hydroxyl radical, Pathophysiology 9 (2003) 215–220.
[178] Y.S. Suzuki, Y. Momose, N. Higashi, A. Shigematsu, K.B. Park, Y.M. Kim, J.R. Kim, J.M. Ryu, Biodistribution and kinetics of holmium-166-chitosan complex (DW-166HC) in rats and mice, J. Nucl. Med. 39 (1998) 2161–2166.
[179] A. Nimrod, E. Ezra, N. Ezov, G. Nachum, B. Parisada, Absorption, distribution, metabolism, and excretion of bacteria-derived hyaluronic acid in rats and rabbits, J. Ocul. Pharmacol. 8 (1992) 161–172.
[180] G. Paradossi, F. Cavalieri, E. Chiessi, C. Spagnoli, M.K. Cowman, Poly(vinyl alcohol) as versatile biomaterial for potential biomedical applications, J. Mater. Sci. Mater. Med. 14 (2003) 687–691.
[181] Z. Grosova, M. Rosenberg, M. Rebros, M. Sipocz, B. Sedlackova, Entrapment of beta-galactosidase in polyvinylalcohol hydrogel, Biotechnol. Lett. 30 (2008) 763–767.
[182] Y. Kaneo, S. Hashihama, A. Kakinoki, T. Tanaka, T. Nakano, Y. Ikeda, Pharmacokinetics and biodisposition of poly(vinyl alcohol) in rats and mice, Drug Metab. Pharmacokinet. 20 (2005) 435–442.
[183] K.M. Koczkur, S. Mourdikoudis, L. Polavarapu, S.E. Skrabalak, Polyvinylpyrrolidone (PVP) in nanoparticle synthesis, Dalton Trans. 44 (2015) 17883–17905.
[184] S. Ahlberg, A. Antonopulos, J. Diendorf, R. Dringen, M. Epple, R. Flock, W. Goedecke, C. Graf, N. Haberl, J. Helmlinger, F. Herzog, F. Heuer, S. Hirn, C. Johannes, S. Kittler, M. Koller, K. Korn, W.G. Kreyling, F. Krombach, J. Lademann, K. Loza, E.M. Luther, M. Malissek, M.C. Meinke, D. Nordmeyer, A. Pailliart, J. Raabe, F. Rancan, B. Rothen-Rutishauser, E. Ruhl, C. Schleh, A. Seibel, C. Sengstock, L. Treuel, A. Vogt, K. Weber, R. Zellner, PVP-coated, negatively charged silver nanoparticles: a multi-center study of their physicochemical characteristics, cell culture and in vivo experiments, Beilstein J. Nanotechnol. 5 (2014) 1944–1965.
[185] R. Si, Y.W. Zhang, L.P. You, C.H. Yan, Self-organized monolayer of nanosized ceria colloids stabilized by poly(vinylpyrrolidone), J. Phys. Chem. B 110 (2006) 5994–6000.
[186] T. Yamaoka, Y. Tabata, Y. Ikada, Fate of water-soluble polymers administered via different routes, J. Pharm. Sci. 84 (1995) 349–354.
[187] R.N. Hardy, The absorption of polyvinyl pyrrolidone by the new-born pig intestine, J. Physiol. 204 (1969) 633–651.
[188] W. Wessel, M. Schoog, E. Winkler, Polyvinylpyrrolidone (PVP), its diagnostic, therapeutic and technical application and consequences thereof, Arzneimittelforschung 21 (1971) 1468–1482.
[189] F. Cabanne, R. Michiels, P. Dusserre, H. Bastien, E. Justrabo, Polyvinyl disease, Ann. Anat. Pathol. (Paris) 14 (1969) 419–439.
[190] C. Couinaud, J. Herve, C. Biotois, J. Gioan, , Polyvinylpyrrolidone thesaurismosis resembling an inflammatory tumor of the great epiploon Sem. Hop. 46 (1970) 3079–3082.
[191] E. Reske-Nielsen, M. Bojsen-Moller, M. Vetner, J.C. Hansen, Polyvinylpyrrolidone-storage disease. Light microscopical, ultrastructural and chemical verification, Acta Pathol. Microbiol. Scand. A 84 (1976) 397–405.

[192] U. Edelmann, P. Johansen, A.B. Pedersen, M. Christensen, C. Hau, , [PVP storage as the cause of specific organ symptoms] Ugeskr. Laeger 139 (1977) 2309–2312.
[193] D.J. Rowe, Letter: alkaline phosphatase levels in epileptic subjects, Br. Med. J. 3 (1974) 686.
[194] T. Yamaoka, Y. Tabata, Y. Ikada, Comparison of body distribution of poly(vinyl alcohol) with other water-soluble polymers after intravenous administration, J. Pharm. Pharmacol. 47 (1995) 479–486.
[195] D. Venturoli, B. Rippe, Ficoll and dextran vs. globular proteins as probes for testing glomerular permselectivity: effects of molecular size, shape, charge, and deformability, Am. J. Physiol. Ren. Physiol. 288 (2005) F605–F613.
[196] A. Besheer, K. Mader, S. Kaiser, J. Kressler, C. Weis, E.K. Odermatt, Tracking the urinary excretion of high molar mass poly(vinyl alcohol), J Biomed Mater Res B Appl Biomater 82 (2007) 383–389.
[197] J.A. Olarte, J.R. Sachetto, J. Vilarino, H.H. Rubio Jr., F.J. Fernandez, Fecal excretion of PVP I-131 in liver cirrhosis, Gastroenterologia 102 (1964) 159–162.
[198] B.P. Hazenberg, L. Arisz, A. van Zanten, E. Mandema, Intestinal excretion of low and high molecular weight polyvinylpyrrolidone (PVP) in patients with proteinuria, Acta Med. Scand. 185 (1969) 515–522.
[199] L. Arisz, B.P. Hazenberg, A. van Zanten, E. Mandema, Renal excretion of low and high molecular weight polyvinylpyrrolidone (PVP) in patients with proteinuria, Acta Med. Scand. 186 (1969) 393–400.
[200] R.K. Loeffler, J. Scudder, Excretion and distribution of polyvinyl pyrrlidone in man, as determined by use of radiocarbon as a tracer, Am. J. Clin. Pathol. 23 (1953) 311–321.
[201] F. Mottaghitalab, M. Farokhi, M.A. Shokrgozar, F. Atyabi, H. Hosseinkhani, Silk fibroin nanoparticle as a novel drug delivery system, J. Control. Release 206 (2015) 161–176.
[202] Y. Cao, B. Wang, Biodegradation of silk biomaterials, Int. J. Mol. Sci. 10 (2009) 1514–1524.
[203] V. Karageorgiou, L. Meinel, S. Hofmann, A. Malhotra, V. Volloch, D. Kaplan, Bone morphogenetic protein-2 decorated silk fibroin films induce osteogenic differentiation of human bone marrow stromal cells, J. Biomed. Mater. Res. A 71 (2004) 528–537.
[204] V. Karageorgiou, M. Tomkins, R. Fajardo, L. Meinel, B. Snyder, K. Wade, J. Chen, G. Vunjak-Novakovic, D.L. Kaplan, Porous silk fibroin 3-D scaffolds for delivery of bone morphogenetic protein-2 in vitro and in vivo, J. Biomed. Mater. Res. A 78 (2006) 324–334.
[205] E. Wenk, H.P. Merkle, L. Meinel, Silk fibroin as a vehicle for drug delivery applications, J. Control. Release 150 (2011) 128–141.
[206] K. Jastrzebska, K. Kucharczyk, A. Florczak, E. Dondajewska, A. Mackiewicz, H. Dams-Kozlowska, Silk as an innovative biomaterial for cancer therapy, Rep. Pract. Oncol. Radiother. 20 (2015) 87–98.
[207] M. Li, M. Ogiso, N. Minoura, Enzymatic degradation behavior of porous silk fibroin sheets, Biomaterials 24 (2003) 357–365.
[208] G.H. Altman, F. Diaz, C. Jakuba, T. Calabro, R.L. Horan, J. Chen, H. Lu, J. Richmond, D.L. Kaplan, Silk-based biomaterials, Biomaterials 24 (2003) 401–416.
[209] A. Biwer, G. Antranikian, E. Heinzle, Enzymatic production of cyclodextrins, Appl. Microbiol. Biotechnol. 59 (2002) 609–617.
[210] O. Adeoye, H. Cabral-Marques, Cyclodextrin nanosystems in oral drug delivery: a mini review, Int. J. Pharm. 531 (2017) 521–531.
[211] C. Aranda, K. Urbiola, A. Méndez Ardoy, J.M. García Fernández, C. Ortiz Mellet, C.T. de Ilarduya, Targeted gene delivery by new folate-polycationic amphiphilic cyclodextrin-DNA nanocomplexes in vitro and in vivo, Eur. J. Pharm. Biopharm. 85 (2013) 390–397.
[212] F. Hirayama, K. Uekama, Cyclodextrin-based controlled drug release system, Adv. Drug Deliv. Rev. 36 (1999) 125–141.
[213] E. Roka, Z. Ujhelyi, M. Deli, A. Bocsik, E. Fenyvesi, L. Szente, F. Fenyvesi, M. Vecsernyes, J. Varadi, P. Feher, R. Gesztelyi, C. Felix, F. Perret, I.K. Bacskay, Evaluation of the cytotoxicity of α-cyclodextrin derivatives on the Caco-2 cell line and human erythrocytes, Molecules 20 (2015) 20269–20285.
[214] Y. Kubota, M. Fukuda, M. Muroguchi, K. Koizumi, Absorption, distribution and excretion of β-cyclodextrin and glucosyl-β-cyclodextrin in rats, Biol. Pharm. Bull. 19 (1996) 1068–1072.
[215] V.J. Stella, Q. He, Cyclodextrins, Toxicol. Pathol. 36 (2008) 30–42.
[216] D.A. Stevens, Itraconazole in cyclodextrin solution, Pharmacotherapy 19 (1999) 603–611.
[217] S.V. Kurkov, T. Loftsson, Cyclodextrins, Int. J. Pharm. 453 (2013) 167–180.
[218] M.A. Phillips, M.L. Gran, N.A. Peppas, Targeted nanodelivery of drugs and diagnostics, Nano Today 5 (2010) 143–159.